Portland State University
PDXScholar

Dissertations and Theses | Dissertations and Theses

2-15-1996

Heme Proton Resonance Assignments and Kinetics Study in High-spin and Mixed-spin Metmyoglobin Complexes by Chemical Exchange NMR Spectroscopy

Ying Luo
Portland State University

Follow this and additional works at: https://pdxscholar.library.pdx.edu/open_access_etds

Part of the Chemistry Commons
Let us know how access to this document benefits you.

Recommended Citation
Luo, Ying, "Heme Proton Resonance Assignments and Kinetics Study in High-spin and Mixed-spin Metmyoglobin Complexes by Chemical Exchange NMR Spectroscopy" (1996). *Dissertations and Theses.* Paper 5238.
https://doi.org/10.15760/etd.7111

This Thesis is brought to you for free and open access. It has been accepted for inclusion in Dissertations and Theses by an authorized administrator of PDXScholar. Please contact us if we can make this document more accessible: pdxscholar@pdx.edu.

THESIS APPROVAL

The abstract and thesis of Ying Luo for the Master of Science degree in Chemistry were presented February 15, 1996 and accepted by the thesis committee and the department.

COMMITTEE APPROVALS: [redacted], Chair

David H. Peyton

[redacted]

Bryant A. Gilbert

[redacted]

Raymond P. Lutz

[redacted]

Pavel K. Smejtek
Representative of the Office of Graduate Studies

DEPARTMENT APPROVAL: [redacted]

David H. Peyton, Chair
Department of Chemistry

* *

ACCEPTED FOR PORTLAND STATE UNIVERSITY BY THE LIBRARY

by [redacted] on 18 March 1996

ABSTRACT

An abstract of the thesis of Ying Luo for the Master of Science in Chemistry presented February 15, 1996.

Title: Heme Proton Resonance Assignments and Kinetics Study in High-Spin and Mixed-Spin Metmyoglobin Complexes by Chemical Exchange NMR Spectroscopy

NMR studies of paramagnetic hemoproteins have improved significantly our understanding of the structure-function relationship of hemoproteins in general. Up to date most of the studies focus on low-spin ferric systems which are characterized by relatively narrow resonance peaks and concomitant better resolution.

However, characterizing in detail the NMR spectra of high-spin ferric hemoproteins is important since there are several hemoproteins, such as peroxidases, catalases, oxygenases, and some ferricytochromes that contain high-spin iron (III) in their biologically active forms. Yet assigning resonances from heme peripheral protons and/or heme pocket residues in high-spin myoglobins is a daunting undertaking. Only a sparse number of active site residues are assigned in such instances, even for metaquo-myoglobin. The protons from the heme and heme pocket

residues in high-spin complexes experience extremely fast relaxation and very broad linewidths, which impede the 2D methods that detect through-space and through-bond connectivities.

It is the intention of this study to develop an effective strategy to gain more resonance assignments for fast-relaxing protons in hemoproteins. We have set out to use a combined strategy, using two-dimensional exchange spectroscopy (2D-EXSY) with two dimensional nuclear Overhauser effect spectroscopy / correlation spectroscopy / total correlation spectroscopy (NOESY/COSY/TOCSY). I demonstrate here that 2D EXSY experiments can be used to obtain assignment correlations for the heme protons of methydroxy-, metthiocyano-, metaquo-, and metimidazole-myoglobin forms. All these assignments are unambiguous and straightforward. Moreover, saturation-transfer experiments allow determination of ligand binding kinetics. Thus, the exchange rates between the metaquo- and metimidazole- or methyl substituted imidazole myoglobin complexes are estimated. The differences between the exchange rates reflect the differences in the hydrophobic and steric interactions between the ligands and the protein moiety. Although I only demonstrate the feasibility of 2D EXSY for the myoglobin case, this assignment strategy should to be applicable to other hemoprotein systems.

HEME PROTON RESONANCE ASSIGNMENTS AND KINETICS STUDY IN HIGH-SPIN AND MIXED-SPIN METMYOGLOBIN COMPLEXES BY CHEMICAL EXCHANGE NMR SPECTROSCOPY

by

YING LUO

A thesis submitted in partial fulfillment of the
requirements for the degree of

MASTER OF SCIENCE
in
CHEMISTRY

Portland State University
1996

ACKNOWLEDGEMENTS

I wish to express my appreciation to a number of individuals who have been invaluable to me throughout this research.

First and foremost, my research advisor, Dr. David H. Peyton, for without his guidance, wisdom and patience, this study would not have been possible.

I am grateful to Dr. Brian A. Gilbert, Dr. Raymond P. Lutz and Dr. Pavel K. Smejtek, who reviewed the thesis and served in my committee.

I would also like to thank Dr. Sydney Yee for the time she spent showing me the techniques employed in the laboratory and intellectual discussions, and Dr. Elisar Barbar, who provided constant support all these years.

I would also like to thank my parents who showed me the wonder of chemistry in my childhood and led me to the door of science, and all the other family members for their endless love and encouragement.

TABLE OF CONTENTS

ACKNOWLEDGEMENTS ii
LIST OF TABLES vi
LIST OF FIGURES vii
ABBREVIATIONS ix

CHAPTER I INTRODUCTION
1. Myoglobin function and structure 3
2. Various myoglobin complexes 5
3. NMR of paramagnetic hemoproteins 6
4. Paramagnetic shifts 6
5. Significant of paramagnetic resonance assignments 7
6. Assignment methods. 8
(1)Deuterium isotope labeling 9
(2)Comparison to model compounds 9
(3)1D NOE 10
(4)1D saturation transfer 11
(5) Conventional 2D methods (NOESY/COSY) 12
(6) 2D EXSY. 13
7. Previous work on the subject 13
(1) Assignment of metMbIm 13
(2) Assignment of metMbH_2O. 14
(3) Assignment of metMbOH. 15
(4) Assignment of metMbSCN 15
(5) Assignment of metMb(1MeIm) and metMb(4MeIm) 15

CHAPTER II METHODS AND MATERIALS

1. Materials 17

2. Instrumentation 18

3. NMR experiments 18

(1) General consideration. 18

(2) 2D EXSY. 20

(3) 2D NOESY/COSY/TOCSY 20

(4) T_1 measurements 22

(5) 1D saturation transfer experiments 23

(6) Exchange rate calculations. 24

CHAPTER III RESULTS AND DISCUSSION

1. Additional assignment of metMbIm by NOESY/COSY/TOCSY 25

2. Additional assignment of metMbH_2O by 2D EXSY. 25

3. Assignment of metMbOH 26

4. Assignment of metMbSCN. 27

5. T_1 comparison 29

6. Spin states 29

7. Linewidth comparison 30

8. Exchange rates 31

CHAPTER IV CONCLUSIONS 34

REFERENCES 36

APPENDIX TABLES 42

APPENDIX FIGURES 46

LIST OF TABLES

TABLE PAGE

I ^{1}H NMR assignments of heme protons in equine metMbH_2O, metMbSCN, metMbOH and metMbIm at 323 K 42

II. T_1s of heme protons of metMbH_2O, metMbSCN, metMbOH and metMbIm, metMb(1MeIm) and metMb(4MeIm) at 323K 43

III. Exchange rates between metMbH_2O and metMbIm, methyl substituted imidazole metmyoglobins. 45

LIST OF FIGURES

FIGURE PAGE

1. Three-dimensional crystal structure of myoglobin 46

2. Comparison of myoglobin and hemoglobin structure 47

3. Structure of heme in myoglobin 48

4. Ligation states in high-spin and low-spin myoglobin complexes 49

5. Electronic states in myoglobin complexes. 50

6. Assignment of methyl protons and vinyl protons by deuterium isotope labeling for metMbH_2O 51

7. Assignment of heme protons by 2D NOESY/COSY experiments in horse heart metMbIm 52

8. Assignment of heme protons by 1D NOE in metMbH_2O 53

9. Assignment of methyl heme protons of equine metMbSCN and metMbOH by 1D saturation transfer 54

10. Assignment of methyl heme protons of equine metMbSCN by deuterium isotope labeling 55

11. Additional assignment of heme protons of metMbIm by 2D NOESY/COSY/TOCSY experiments 56

12. 2D EXSY spectrum of metMbIm: metMbH_2O mixture to gain extra assignments of metMbH_2O 57

13. 2D EXSY spectrum of metMbIm / metMbOH mixture 58

14. Acid to base transition of equine metmyoglobin 59

15. 2D EXSY spectrum of metMbOH / metMSCN mixture 60

16. 1H NMR spectrum of metMbH_2O/metMbF and metMbOH/metMbF mixtures 61

17. T_1 experiment of metMbH_2O at 323K 62

18. T_1 experiments of metMbOH at 323K 63

19. T_1 experiments of metMbSCN at 323K 64

20. T_1 experiments of metMbIm at 323K 65

21. T_1 experiments of metMb(1MeIm) at 323K 66

22. T_1 experiments of metMb(4MeIm) at 323K 67

23. Examples of plots for T_1 determinations 68

24. 1D saturation transfer experiment in metMbH_2O / metMbIm mixture at 323K 69

25. 1D saturation transfer experiment in metMbH_2O / metMb(4MeIm) mixture at 323K. 70

26. 1D saturation transfer experiment in metMbH_2O / metMb(1MeIm) mixture at 323K 71

27. Linewidth comparison among myoglobin complexes 72

28. Structures of imidazole and methyl substituted imidazoles bound to myoglobin 73

ABBREVIATIONS

Hb	hemoglobin
Im	imidazole
1MeIm	1-methyl imidazole
2MeIm	2-methyl imidazole
4MeIm	4-methyl imidazole
Mb	myoglobin
met	myoglobin in iron (III) state
metMbCN	met-cyano myoglobin
metMbIm	met-imidazole myoglobin
metMb(1MeIm)	metmyoglobin complex with 1-methyl imidazole
metMb(2MeIm)	metmyoglobin complex with 2-methyl imidazole
metMb(4MeIm)	metmyoglobin complex with 4-methyl imidazole
$metMbH_2O$	met-aquo myoglobin
metMbOH	met-hydroxyl myoglobin
metMbSCN	met-thiocyano myoglobin
COSY	Correlation SpectroscopY
EXSY	Exchange SpectroscopY
NOESY	Nuclear Overhauser Effect SpectroscopY
TOCSY	Total Correlated SpectroscopY
TPPI	time-proportional phase incrementing

CHAPTER I

INTRODUCTION

Myoglobin Function and Structure

Myoglobin (Mb) is an oxygen transport and storage protein. It plays vital roles in one of the most important aspects of animal metabolism - the acquisition and utilization of oxygen. The most efficient energy-generating mechanisms in animal cells require molecular oxygen for the oxidation of foodstuffs. Therefore, proteins that deliver oxygen to cells and store it until needed are essential for any higher organism. Mb is found in virtually all higher animals, especially in tissues such as muscle, which require large oxygen reserves for periods when energy demands are high. The rate that oxygen can diffuse from the capillaries to tissues, and thus the level of respiration, is limited by the oxygen's low solubility in aqueous solution. Mb increases the effective solubility of oxygen in muscle. Mb functions as a kind of molecular bucket brigade to facilitate oxygen diffusion.[1,2] In animals with a circulatory system, the oxygen transport function is performed by both hemoglobin (Hb) and Mb: Hb carries oxygen from the lungs to tissues via the circulatory system, and Mb binds the cellular oxygen and releases it when it is required for metabolic processes. Hb binds oxygen more easily in the lungs and releases it to myoglobin in the tissues owing to allosteric

effects from low oxygen pressure, low pH resulting from high concentration of dissolved CO_2, and from high chloride ion concentration.[1,2]

Human (or equine) Mb is a small monomeric protein of 153 amino acids with a single iron protoporphyrin(IX), or heme group. Mb's three-dimensional structure is illustrated in Figure 1. Hb, on the other hand, is a tetramer with two pairs of identical subunits labeled α and β; each subunit binds an oxygen molecule. Figure 2 compares the x-ray crystal structures of myoglobin and hemoglobin. Each of the four chains in hemoglobin has a folding structure similar to that of myoglobin. The Hb α and β chains are very similar but are distinguishable in details of both primary structure and folding.

Mb and Hb belong to a large protein family termed hemoproteins, which contain various iron-porphyrin ligands as prosthetic groups in the protein structures. The functions of hemoproteins vary widely and include: (1) oxygen binding and transport (Mb, Hb), (2) transfer of electrons (redox proteins and enzymes, such as cytochromes), (3) insertion of oxygen atoms or dioxygen into organic substrates (cytochrome P-450, cytochrome H-450, chloroperoxidase), and (4) catalysis of other important organic reactions (cytochrome c oxidase, cytochrome c peroxidase, horseradish peroxidase). Owing to its relatively small size and high stability, myoglobin has served as a model for studying protein-ligand interactions, and structure-functional relationships in hemoproteins and proteins in general.[3-5]

Various Complexes in Mb

The structure of the prosthetic group, heme in Mb is shown in Figure 3. The key feature of the porphyrin is the presence of a relatively rigid macrocyclic tetradentate ligand which is nearly planar. The removal of heme from Mb is facile at low pH, as is the reconstitution of apomyoglobin with modified hemes at neutral or higher pH.

Many of the properties of paramagnetic Mb depend upon the status of heme iron ion coordination. The coordination structures and oxidation states that commonly occur in Mb are indicated in Figures 4 and 5. In Mb, the naturally occurring iron oxidation state is ferrous (Fe^{2+}): the protein is either in the deoxygenated form (deoxy) with four unpaired electrons, or in the oxygenated state (oxy) which is a diamagnetic form. The iron is coordinated with the four heme pyrrole nitrogens and the proximal histidine N_ε (Figure 4). Carbon monoxide can also bind to ferrous Mb or Hb to yield 6-coordinate diagmagnetic forms (Figure 4). In deoxyMb the iron does not lie within a plane defined by the heme pyrrole nitrogens, but projects out of the heme plane toward the proximal histidine.[6] Although usually not as pronounced, the ferric (Fe^{3+}) oxidation state of most heme proteins also exhibits this out-of-plane displacement in the unligated (5-coordinate) state.[6]

Physiologically, Mb can be irreversibly oxidized to the metmyoglobin form, which contains high-spin iron(III). Upon binding a strong ligand, such as cyanide ion, the ferric protein is converted to the low spin (S=1/2) state. This electronic state has

only a single unpaired electron as shown in Figure 5B. Thus, the ligated, 6-coordinate state appears in ferrous and ferric forms of myoglobin. Crystallographic data reveal that in this type of structure the iron ion lies in the plane of the porphyrin ring. Neglecting the fact that the ligands are different, the local structure is best described by a distorted octahedrally coordinated iron ion, albeit with different ligands.

For ferric proteins capable of ligand binding, several species are capable of being bound at the sixth coordination site, yet do not produce sufficiently strong ligand fields to convert the heme iron completely to the low-spin state. These intermediate or mixed-spin states (Table I) are induced by such ions as SCN^-, N_3^-, Im and OH^-. Current reviews exist that discuss the concept of mixed-spin porphyrin systems and their origin.[7-9]

Nuclear Magnetic Resonance Spectroscopy(NMR) of Paramagnetic Heme Proteins

NMR has played a key role in delineating structure-function relationship in hemoproteins.[6,10-12] The characteristic NMR parameters for paramagnetic states are (1) spreading of the chemical shift range; (2) short T_1; and (3) short T_2 leading to large linewidth. These large perturbations are due to the interaction between the proton nuclei and the unpaired electron(s) residing on the heme iron.[6]

Paramagnetic Shifts

In the presence of unpaired electrons in a molecule, the observed chemical shifts are contributed by both diamagnetic and paramagnetic shifts.[12-14] The diagmagnetic shift arises from the shielding of the nucleus from the external magnetic shift as a result of the electron density around, and the circulation of the electrons near the nucleus itself. The paramagnetic, or hyperfine, shift is the difference between the chemical shift of a given nucleus in the paramagnetic molecule and what its shift would be in a diamagnetic molecule of the same structure.

$$\delta_{obs} = \delta_{dia} + \delta_{para} \quad (1)$$

There are two contributions to the paramagnetic shift or hyperfine shift, the contact and dipolar (pseudocontact) terms.[12-14]

$$\delta_{para} = \delta_{con} + \delta_{dip} \quad (2)$$

The contact shift (δ_{con}) has its origin in scalar coupling between electron spins and a given nucleus. The dipolar, or pseudocontact, contribution to the paramagnetic shift results from through-space dipole-dipole coupling of the nuclear and electron magnetic moments. Contact shifts provide details of covalent bonds to the iron, while dipolar shifts provide both molecular structural details for noncoordinated amino acid residues and information about the magnetic properties of the iron. This wealth of information in the hyperfine shift, however, becomes accessible only upon first unambiguously assigning the hyperfine-shifted resonances in a paramagnetic protein.

Significance of Resonance Assignments

The hyperfine-shifted resonance as a result of interactions between proton nuclei and the paramagnetic heme iron have been investigated to gain insight into the electronic structures of the heme embedded in the polypeptide chain of the protein.[12] The initial, critical step for protein structure analysis demands definitive resonance assignments of nearby residues. For hemoproteins, the resonance assignment assumes an even greater importance, because it forms the basis for understanding both the solution-state structure and the electronic properties of the heme iron. The hyperfine-shifted signals reflect the electronic structure and can, in particular, elucidate the orbital ground state.[16] As a result, structural perturbations that alter the electronic state are often manifested in the hyperfine chemical shift pattern, which points to the molecular mechanisms controlling ligand binding affinity.[13]

Assignment Methods

Although there are some aspects of solution behavior of hemoproteins that can be studied in the absence of assignments, when specific resonance assignments can be made for a given protein a barrier to detailed understanding of the molecular level events accompanying the protein's function is surmounted. The following methods can be used to make unambiguous resonance assignments for the heme and nearby residues.

1. Specific deuterium labeling

Specific deuterium labeling of iron protoheme IX and subsequent reconstitution into Mb has been the most reliable and most widely used method for making unambiguous assignments of heme protons. Although the procedures are well known, they are time-consuming and arduous. The synthetic work[17-20] of G.W. Kenner, Kevin Smith, and their co-workers has contributed significantly to our understanding of heme protein function since 1978. The ferric high-spin proteins have large paramagnetic shifts of protons of the heme group. Consequently, unambiguous assignments can be made for all the heme methyl groups, most vinyl protons, and in fortuitous cases, the *meso* protons, as illustrated in the Figure 6.

2. Comparison to model compounds

Since before the use of isotopically enriched hemes, model systems have played a major role in interpreting heme protein NMR spectra.[10] The use of iron porphyrin model systems in making resonance assignments in heme proteins has been reviewed.[7,610,23,24] Models can be used in the least refined approximation to illustrate how spectra of particular types of well characterized iron porphyrins should appear in comparison with actual heme protein spectra. An illustration of this method is the vinyl proton assignment made in met-myoglobin cyanide, which is based on the Curie behavior ($\delta_{para} \propto 1/T$) of the spectrum of low spin ferric porphyrin models.[21-22]

3. 1D NOE

The one-dimensional nuclear Overhauser effect (1D NOE), is defined as a change in the resonance intensity of a nuclear spin when the resonance of another spin is saturated. The NOE originates from dipole-dipole interactions between pairs of nuclear spins. Random molecular motions at the resonance frequency of the magnetic moments of spins at one site induce magnetic transitions in the spins at another site. The net effect is the exchange of magnetization between the sites. The NOE's magnitude is proportional to the reciprocal of the sixth power of the distance between the irradiated and the observed nucleus. The magnitude of NOE also depends on the correlation time for the interaction between the two protons. NOE represents one of the most powerful techniques for peak assignment as well as for solution structure determination in highly folded biopolymers.[25-26] It had generally been assumed that the unpaired electron(s) in a molecule would obviate any NOE; consequently, for a long time no investigation was attempted on paramagnetic systems. Not until the early 1980s have data become available to demonstrate NOEs can be used for making important assignments in a variety of paramagnetic proteins.[27] However, NOE detection by 1D NOE experiments has its limitations: (1) the lines in paramagnetic molecules are difficult to saturate due to short T_1s, thus a decoupler with high rf power is necessary; a strong rf pulse induces large off-resonance effects which could make

true NOEs difficult to be distinguished from artifacts; (2) the saturation pulse can be used to irradiate only well-resolved resonances.

4. 1D saturation Transfer

1D saturation transfer[28] is used to relate pairs of signals belonging to the same nuclear species in two different chemical environments in the presence of moderately slow chemical exchange. Two separate signals are observed under this condition. Chemical exchange, in the NMR sense, reflects all processes of inter- and intramolecular rearrangements in which observed spins change their magnetic environment. In NMR spectroscopy, slow refers to an exchange rate k_{ij} between sites i and j that is smaller than the difference in resonance frequencies (in Hz) of the two exchange sites; that is, exchange that is slow enough not to cause the individual resonances to coalesce into a single line: $k_{ij} << |\omega_I - \omega_j|/2\pi$. The lower limit of the exchange processes is imposed by T_1 relaxation of the spins. To be observed, the rate of the exchange process must be greater than or comparable to the T_1 relaxation rate ($1/T_1$): $k_{ij} \geq R_i, R_j$, where $R_i = 1/T_{1i}$. Chemical exchange processes in proteins include all internal rearrangements, such as slow side-chain rotations or reversible folding, and reversible intermolecular interactions, such as exchange of labile protons or bimolecular associations. These processes, when exhibit much higher rates than can be studied by exchange spectroscopy ($k_{ij} \geq |\omega_I - \omega_j|/2\pi$.), can be investigated by NMR relaxation time measurements or line shape analysis.

Although 1D saturation transfer can be analyzed simply, it suffers from several shortcomings: (1) the exchange rate has to fit in the suitable range to be slow on the NMR time scale, yet greater than the relaxation rate ($1/T_1$); (2) saturation can induce off-resonance effects; (3) only the well-resolved resonances can be saturated.

5. Conventional 2D methods (NOESY/COSY)

Two-dimensional nuclear Overhauser effect spectroscopy (NOESY)[29] and correlation spectroscopy (COSY)[30-31] have been recognized to be very power tools to achieve resonance assignments and three-dimensional structures of biopolymers in the last decade.[32] Whereas the NOESY experiment detects through-space interactions, identifying pairs of protons that are within 5 Å of one another, the COSY experiment detects through-bond interactions, elucidating the direct J-coupling of two protons, thereby assisting in sorting proton resonances by residues. 2D NOESY/COSY methods have allowed successful assignments for heme and/or heme pocket residue resonances in low-spin metcyano-myoglobin (metMbCN),[33] aplysia metcyano-myoglobin,[34] horse heart cytochrome c[35] and mixed-spin metazido-myoglobin.[36] For the high-spin or mixed-spin systems with large high-spin content, the mixing times have to be shorter than the relaxation times of the protein complexes. For instance, the relaxation times of heme resonances in $metMbH_2O$ are in the range of ~ 2-20 msec, which is too short to detect conveniently the coherence transfer during the mixing time of NOESY spectra.

6. 2D EXSY

To solve the problem of not being able to use conventional 2D NOESY/COSY method for wholly and essential high-spin hemoproteins, I demonstrate in this study a combined strategy: 2D exchange spectroscopy (2D EXSY) in combination with 2D NOESY/COSY. 2D exchange spectroscopy (2D EXSY)[37] has been recognized to be very useful to study the dynamic processes in liquids. 2D EXSY is the 2D version of the 1D saturation transfer experiment, still requiring the same restriction in exchange rates in the systems to be able to apply this technique[35]. However, 2D EXSY has the following advantage over the 1D experiment: (1) it avoids using decoupling power to saturate individuals peaks, giving no off-resonance effects; (2) it provides much greater resolution because the peaks are spread into the second dimension; (3) all the saturation transfer peaks are obtained at once, so the experiment is more convenient to set up the experiment and to analyze data. Also, the data are more easily viewed in the 2D plot than in a long series of 1D difference plots.

Previous work on the subject of this study

1. Assignment of metMbIm

Many assignments of metMbIm were achieved by NOESY/COSY in a previous work:[40] phase sensitive NOESY and magnitude COSY for metMbIm in ^2H_2O at 31°C and pH 6.8 are shown in Figure 7. Three heme methyls are first recognized by

their well resolved hyperfine-shifted positions with integrals of three protons relative to other resonances of single proton intensity. The assignment process is made based on the through-space and through-bond connectivities, starting from the NOE between $8CH_3$ and $1CH_3$, the only heme methyls close enough to have an NOE between them. The $8CH_3$ and $1CH_3$ are distinguished by the $1CH_3$ NOE to a vinyl spin system. 2-vinyl group was recognized by its characteristic AMX spin systems with the J-coupled connectivities ($2H_\alpha$; $2H_{\beta t}$), ($2H_\alpha$; $2H_{\beta c}$), ($2H_{\beta}t$; $2H_{\beta c}$). The 2-vinyl group has NOE to the $1CH_3$ ($1CH_3$; $2H_\alpha$), ($1CH_3$; $2H_{\beta t}$), ($1CH_3$; $2H_{\beta c}$). The 6-propionate was assigned by its NOE to $5CH_3$ and it produced many of the possible COSY/NOESY cross peaks: ($6H_\alpha$; $6H_\alpha'$), ($6H_\alpha$; $6H_\beta$), ($6H_\alpha$; $6H_\beta'$), ($6H_\alpha'$; $6H_\beta$), ($6H_\alpha'$; $6H_\beta'$), ($6H_\beta$; $6H_\beta'$).

2. Assignment of metMbH_2O

The heme proton resonances of metMbH_2O were assigned by deuterium isotope labeling[41] and 1D NOE[27] experiments as indicated in Figure 6 and 8. La Mar and his co-workers demonstrated that the1D NOE is effective for making assignments in the high-spin (S=5/2) ferric met-aquo myolobin, metMbH_2O, which has efficient paramagnetic contribution to nuclear relaxation; and yet its spectrum is relatively well-resolved by virtue of large hyperfine shifts. With a number of the heme resonances first assigned by isotope labeling, the propionate peak assignments were obtained by

saturating $8CH_3$ and $5CH_3$ to gain assignments of $7H_\alpha$, $7H_\alpha$', $6H_\alpha$; saturating $7H_\alpha$ and $6H_\alpha$ gains assignment to $7H_\beta$ and $6H_\alpha$, respectively.

3. Assignment of metMbOH

There are two kinds of methods reported for assigning the heme protons of metMbOH. Sperm whale metMbOH was assigned by deuterium isotope labeling method by reconstituted apomyoglobin with (1,5-$^2H_6$) heme and (1,3-$^2H_6$) heme.[42] The 1D saturation transfer method was used by Yamamoto to obtain the limited assignments for metMbOH, as shown in Figure 9 A-D.[43]

4. Assignment of metMbSCN

The situation of heme proton assignment of metMbCN is similar situation to metMbOH. There are two methods reported for assigning the heme protons of metMbSCN. Three methyl groups of sperm whale metMbSCN were assigned by deuterium isotope labeling method by reconstituted apomyoglobin with (1,5-$2H_6$) heme and (1,3-$2H_6$) heme.[42] The 1D saturation transfer method was used by Yamamoto[43] to obtain the assignment for metMbSCN, as shown in Figure 9 E-I.

5. Assignment of metMb(4MeIm) and metMb(1MeIm)

The same strategy in assigning metMbIm resonances was used to make assignments for the heme protons of the methylated Mb complexes. Eleven assignments were obtained for both complexes in a previous work.[40]

CHAPTER II

MATERIALS AND METHODS

MATERIALS

Horse heart metmyoglobin was purchased from Sigma as lyophilized powder and dissolved in 50 mM phosphate, 150 mM NaCl buffer in D_2O solution. The total concentration of the protein was 4 mM for each sample. All the external ligands (L) added were reagent grade, and the molar ratios of two metmyoglobin complexes were about 1:1. Ratios were monitored by ^1H NMR. The mixtures for 2D EXSY experiments were prepared as followings: a mixture of metMbIm and metMbH_2O was prepared by adding aliquots of imidazole in D_2O solution to 4 mM slightly acidic myoglobin solution in 50 mM phosphate, 0.1M NaCl buffer (pH 6.8) in D_2O to achieve ~ 1 :1 ratio of each species. A mixture of metMbIm and metMbOH was prepared by adding aliquots of imidazole D_2O solution to 4 mM basic myoglobin solution (pH 10.6) in 50 mM phosphate, 0.1M NaCl buffer in D_2O until ~ 1:1 ratio of each species is reached; a mixture of metMbSCN and metMbOH was prepared by adding aliquots of KSCN D_2O solution to 4 mM basic myoglobin solution (pH 10.6) in 50 mM, 0.1M NaCl buffer in D_2O until ~ 1:1 ratio of each species is reached. The pH values were uncorrected for the isotope effect.

INSTRUMENTATION

Proton NMR spectra were recorded on a Bruker AMX 400 spectrometer interfaced with Aspect X32 computer and equipped with a dedicated 5 mm ^1H probe. Chemical shifts are referenced to 2, 2-dimethyl-2-silapentane-5-sulfonate (DSS) through the residual water resonance.

NMR EXPERIMENTS

In this study, I utilize the following exchange reactions:

$$metMbH_2O + Im \Leftrightarrow metMbIm + H_2O \quad (3)$$

$$metMbH_2O + 1MeIm \Leftrightarrow metMb(1MeIm) + H_2O \quad (4)$$

$$metMbH_2O + 4MeIm \Leftrightarrow metMb(4MeIm) + H_2O \quad (5)$$

$$metMbH_2O + SCN^- \Leftrightarrow metMbSCN + H_2O \quad (6)$$

$$metMbOH + Im \Leftrightarrow metMbIm + OH^- \quad (7)$$

$$metMbOH + SCN^- \Leftrightarrow metMbSCN + OH^- \quad (8)$$

These exchange rates fall in the range suitable for observation by NMR, which enables us to assign the hyperfine-shifted resonances by using 2D EXSY experiments. EXSY also provides a highly sensitive approach to investigate the dynamics of heme cavity in the high-spin and low-spin complexes of metmyoglobin.

1. General Considerations[44]

To cover a large range of chemical shifts, it is important to use short exciting pulses and a fast analog-to-digital converter (ADC). Short T_1 values for the resonances of interest allow faster scanning and therefore high signal-to-noise ratios for a given experiment time. On the other hand, short T_2 values imply large linewidths, and the S/N is inversely proportional to the linewidth.

Proper choice of the magnetic field is a prerequisite considering all the field-dependent paramagnetic effects on T_1 and T_2. In the absence of these effects the obvious choice would be the highest magnetic field available, since both resolution and sensitivity increase almost linearly with magnetic field. T_1^{-1} goes ultimately to zero at high magnetic field, whereas T_2^{-1} levels off at a field-independent value. Therefore, it is advisable not to choose too high a field because this may result in a longer T_1 (slower scanning with no improvement in linewidth). Even though relaxation rate arising from chemical shift anisotropy is proportional to the square of the applied magnetic field, this effect does not cause line broadening for proton nuclei at high applied fields.

Another general phenomenon that should be considered in paramagnetic macromolecules is the occurrence of Curie spin relaxation. The line broadening introduced by this relaxation mechanism is proportional to the square of magnetic field, and therefore becomes dramatic at very high fields. The onset of such a mechanism as the dominant one depends on the relative values of the electronic and rotational correlation times, as well as the number of unpaired electrons on the metal

ion. For metMb complexes, our instrument Bruker AMX 400 with magnetic field at 9.4 Telsa compromises spectral resolution and these different effects.

2. 2D EXSY

Two dimensional phase-sensitive EXSY spectra were acquired using the standard NOESY pulse sequence:[30,37]

relaxation delay - 90° - t_1- 90°- t_m - 90° - FID (t_2)

Quadrature detection in t_1 was achieved using time-proportional phase increase (TPPI).[45] The mixing time of 5 msec was chosen, which was long enough to obtain sizable EXSY cross peaks, while avoid the problems of NOESY cross peak buildup. Typically 256 scans were accumulated for each value of t_1; 300 t_1 values were recorded with free induction decays of 1024 data points. These were then zero filled to 1024 x 1024 real data sets.

All the EXSY spectra were performed at the elevated temperature of 323K to enhance the chemical exchange processes because the chemical exchange rates increase with temperature. Although the metMb complexes are not stable for long periods of time at this temperature, the acquisition times for these experiments are only a few hours at most. The relaxation delay was 500 msec for all the EXSY experiment.

3. 2D NOESY/COSY/TOCSY

Two dimensional magnitude COSY (MCOSY) spectra was acquired using standard methods and phase cycling:[31,46]

relaxation delay - 90° - t_1 - 90° - FID (t_2)

Phase-sensitive NOESY were acquired using the standard pulse sequence:

relaxation delay - 90° - t_1 - 90° - τ_m - 90° - FID (t_2)

the mixing time (τ_m) was 25 msec. A short relaxation time (20 msec) was used in order to obtain large collection of data in a short experiment time. The mixing time of 25 msec gave rise to large NOESY cross peaks between heme protons. These experiments were typically run at 304 K. The temperature was chosen at which metMbIm gives well-resolved 1D hyperfine-shifted resonances, and because at this temperature the protein structure is stable during the relatively long NMR experiments.

Two-dimensional total correlation spectroscopy (TOCSY)[47] was acquired with pulse sequence:

relaxation delay - 90° - t_1 -SL_x - Mlev17 - SL_x - FID (t_2)

in which SL_x denotes a short 2 msec spin lock field applied along the x axis and Mlev 17 is a composite pulse sequence that also spin-locks the protons. TOCSY spectra display both direct and relayed connectivities within a spin system, and are very useful for elucidation of scalar-coupling network. Its advantage is that it gives the entire spin system and coherence transfer is efficient and data are largely pure phase. The intensities of peaks depend on the length of the spin lock mixing time. For metMbIm,

the mixing time of 25 msec was used. 90° pulse for spin lock was calibrated as 21 μs with spin lock power attenuation of 12 dB.

4. *T_1 measurements*

The nonselective T_1s of the resolved resonances of the myoglobin complexes were obtained by inversion recovery experiment by the method of Harris[48] using the pulse sequence:

relaxation delay - 180°- t_D - 90° - FID

where 180° pulse is used to inverse the magnetization, 90° pulse (read pulse) was used to monitor the state of magnetization, and t_D was the delay time between the 180° and 90° pulses, ranging from 0.2 msec to 1 sec. The intensity at 1 sec is regarded as the intensity at infinity since the magnetization has return to its equilibrium position even before this delay time. The natural logarithm of the peak intensity for each peak may be plotted against t_D, and thus T_1 found according to the following equation:

$$\ln(I_\infty - I_t) = \ln 2 + \ln I_\infty - t_D / T_1 \qquad (7)$$

A plot of $\ln(I_\infty - I_t)$ vs t_D was used to determine T_1s of the heme protons of the Mb complexes. T_1 values were thus calculated from the slope ($-1/T_1$).

The spin lattice relaxation times of the resonances in proximity to the paramagnetic center, such as heme methyls, can be determined through a non-

selective, hard 180° inversion pulse. For these resonances, relaxation by the unpaired electrons overwhelms all other mechanisms, so that the T_1s obtained through either selective or nonselective inversion pulse are approximately the same.[47]

5. 1D Saturation Transfer

1D saturation transfer experiments were carried out for mixtures of (1) metMbH_2O-metMbIm; (2) metMbH_2O-metMb(1MeIm); and (3) metMbH_2O-metMb(4MeIm) mixtures respectively. The irradiated methyl peaks are strongly relaxed, hence the use of high rf power, possibly inducing off-resonance effects, was necessary to saturate the peak. To alleviate the problem, lower power irradiation of the methyl was attempted although less than 100% saturation was achieved. The experimental conditions for these three mixtures are exactly the same: power attenuation level of 40 dB and irradiation time of 200 msec were used. The pulse sequence of zgh2pr was utilized with on- and off-resonance frequencies alternating for 64 cycles at 323 K. The pulse sequence is given as follows:

relaxation delay - 90° - acquisition

decoupler on - off

6. Exchange rates

For reactions 3, 4, 5 and 6 the reverse reactions are pseudo-first order, because the concentration of water is essentially constant. The exchange rate k_{-1} can be estimated by[50]

$$k_{-1} = T_1^{-1}\frac{1-F}{F} \tag{10}$$

$$F = I/I_0 \tag{11}$$

where T_1^{-1} is the spin lattice relaxation rate of the interested proton in metMbH_2O. F is saturation factor, which is the ratio of the intensities of the involved resonance with (I) and without t(I_0) irradiation of imidazolate myolgobins determined by 1D saturation transfer experiments. To determine k_{-1} from Equation 10 directly it is required that magnetization of the irradiated peak be reduced to zero,[50-51] i.e. the peak has to be completely saturated. Therefore, I used the difference spectra to normalize the irradiated peaks in order to calculate the saturation factors.

CHAPTER III

RESULTS AND DISCUSSION

1. Additional Assignments of metMbIm by NOESY/COSY

Efforts were taken to achieve more complete assignments of metMbIm than previously available, as shown in Figure 11. The γ *meso* proton at 11.4 ppm was identified by its NOE to $7H_{\alpha}$, $6H_{\alpha}$, $6H_{\alpha}'$, and its broad linewidth (~160 Hz) and an intensity of one proton. The α *meso* proton at 9.62 ppm is identified by its NOE to the $2H_{\alpha}$ and $3CH_3$, and its large linewidth of about 77 Hz. A resonance at 7.42 ppm is identified as the β meso proton based on the NOEs from this proton to the $5CH_3$ and IleFG5$C_{\delta}H_3$. All these distances are consistent with the by x-ray crystal structure of sperm whale myoglobin. 4-vinyl β protons are identified by their AMX spin systems of the vinyl group in TOCSY experiment: ($4H_{\alpha}$, $4H_{\beta c}$), ($4H_{\alpha}$, $4H_{\beta t}$). The small $4H_{\beta t}$-$4H_{\beta c}$ coupling fails to yield a cross peak due to the line width and small value of the coupling constant $J < 2$ Hz.[33] The results are summarized in Table I.

2. Additional Assignments of metMbH_2O by 2D EXSY

Figure 12 shows the downfield hyperfine-shifted region of a phase-sensitive 2D EXSY spectrum of ~1 : 1 mixture of the equine myoglobin complexes: metMbH_2O and metMbIm, recorded at 400 MHz, 50°C, and pH 6.2. The upfield region of the 2D EXSY experiment is shown in the insert. The mixing time was 4 msec and the relaxation delay was 40 msec. The assignments on the horizontal and vertical axes are those of metMbH_2O and metMbIm, respectively. The *meso* γ of metMbH_2O was obtained from the EXSY cross peaks, which matched one of the three unspecified meso protons that were identified by La Mar;[42] A resonance at -5.8 ppm was assigned to $2H_{\beta c}$, which was only able to identified as vinyl β proton.[42] The results are summarized in Table I.

3. Assignments of metMbOH by 2D EXSY

Figure 13 shows the downfield hyperfine-shifted region of phase-sensitive 2D EXSY spectra of ~ 1 : 1 equine metMbOH and metMbIm complexes, recorded at 50°C and pH 10.3, with a mixing time of 5 msec and relaxation delay of 60 msec. The original data matrix was 512 x 512 data points, zero-filled to 1024 x 512. Each block was 300 scans. The running time was 4.5 hrs. Twelve heme protons of metMbOH were assigned through the 2D EXSY cross peaks, based on the corresponding resonances of metMbIm. As the pH of metMbH_2O solution is increased, more

population of this acidic form converts to metMbOH (acid-base transition, illustrated in Figure 14). The exchange rate of metMbOH and metMbH_2O is on the order of 10^5-10^6 s^{-1}, fast on the NMR time scale. The fast exchange rate is due to the association and dissociation of a proton on the ligand (water), which does not require the ligand diffuse out of the heme pocket.[51-52] Thus, the heme resonances in metMbOH can not be assigned directly through the exchange of the acidic and basic form of metaquo-myoglobin. Yet they are easily attainable through the 2D EXSY experiment, as illustrated in Figure 13. The results are included in Table I. This single experiment allows twelve assignments of the heme resonances of metMbOH, which is quite profitable compared to the isotope labeling method which assigned only four methyl heme protons, as shown in Figure 9 E-I. Although the heme resonances of metMbIm change slightly with pH, the assignments of metMbOH are unambiguous because the assignments of metMbIm resonances which correlate with the resonances of metMbOH, are definitive.

4. Assignments of metMbSCN by 2D EXSY

Figure 15 illustrates the downfield hyperfine shifted region of a ~1:1 mixture of metMbSCN and metMbOH at pH 10.3 and 323 K. The mixing time was 5 msec and the relaxation delay was 20 msec. The spectrum was collected in 2 hrs as a 512 x 300 data point matrix. The assignments of heme proton resonances had proved very

difficult to make either by isotope labeling method or 1D saturation-transfer experiment (Figure 9 A-D and 10). Only three methyl protons were assigned by both methods. Nevertheless, our study demonstrates that the heme resonances of metMbSCN are obtained through the cross peaks of a 2D EXSY spectrum of ~1:1 metMbSCN-metMbOH mixture, after the heme resonances of metMbOH are assigned. Nine heme protons are able to assigned, among which the three methyl assignments were consistent with previous work.[43]

An unsuccessful attempt was made to observe 2D-EXSY between metMbH_2O-metMbSCN. Cross-peaks were not detected even though these species exchange slowly enough relative to the NMR time scale to give separate resonances for the mixture, and 1D saturation transfer was able to detect the magnetization transfer from the three methyls.[43] This failure was probably due to the extremely short T_1 values (the T_1's of $5CH_3$ of metMbSCN, metMbH_2O are 4 msec and 4.7 msec, respectively).[40,47]

Likewise, both metMbH_2O and metMbOH exchange with metMbF slowly, yet the 2D EXSY experiments failed to detect the any EXSY cross peaks. This is not surprising because F^- is a weaker ligand to replace the water and OH^- in the reactions. Therefore exchange rates are probably much slower relative to their very fast spin lattice relaxation rates.

5. T_1 Comparison

The inversion-recovery experiments of the myoglobin complexes are illustrated in Figure 17-22. T_1 values were extrapolated from the experiments using Equation 7, using Figure 23 as an example. The results are tabulated in Table II. The wholly and essentially high-spin complexes have very short spin lattice relaxation times compared to the essentially low-spin complexes. These values provide the clues for the difficulties to perform 2D NOESY experiments of metMbH_2O, metMbSCN and metMbOH since the mixing times of NOESY are required to be shorter than T_1 values of each complex, which is too short to detect any coherence transfer.

6. Spin States

According to magnetic property studies,[53-56] metMbSCN was believed to be essentially high-spin, as is metMbH_2O, metMbIm and metMbN_3 were approximately 80 % low-spin, and metMbOH was about 30 % low-spin. Since high spin contents are manifested by the chemical shift dispersion and the spin lattice relaxation rates, the high-spin contents can be calculated from Equation12 and 13,[57] listed in Table I.

$$f^{HS} = (\delta^{obs} - \delta^{LS}) / (\delta^{HS} - \delta^{LS}) \qquad (12)$$

$$f^{HS} = (R_1^{obs} - R_1^{LS}) / (R_1^{HS} - R_1^{LS}) \quad (13)$$

where δ^{HS} (or R_1^{HS}) is the chemical shift (or spin lattice relaxation rate $R_1 = 1/T_1$) of a specific group (i.e., the average of the heme methyls) in the pure high-spin form ($metMbH_2O$), δ^{LS} (or R_1^{LS}) is the chemical shift (or R_1) of the same group in the pure low-spin form (metMbCN), and δ^{obs} (or R_1^{obs}) is the observed chemical shift (or R_1) of the group in the mixed spin case. At 323 K, the δ^{HS} is 73.1 ppm and δ^{LS} is 14.7 ppm obtained from our experimental data at this temperature based on the results.[27,33,41] Despite the discrepancy in the exact values, the four categories they fit into estimated by the three methods are identical.

9. Linewidth Comparison

The broadness of linewidth of metmyoglobin complexes follow the order of $metMbH_2O$ > metMbSCN > metMbOH > metMbIm > $metMbN_3$ > metMb(1MeIm), metMb(4MeIm) > metMbCN, which correlates the order of their high spin contents, with the exception that metMbIm is abnormally broad. In the methylated imidazolate complexes, the linewidths are much narrower, suggestive that the extra methyl group generates more stability of the heme pocket through hydrophobic interaction with the protein matrix, or steric hindrance for the rotation of the imidazole ring. This unusual line broadness in metMbIm likely results from the chemical shift average of the resonances by rotating imidazole ligand around its pseudo-C_2 axis in the heme pocket.

The detailed dynamics in the imidazole and methyl-substituted imidazole complexes of metmyoglobin has been studied.[40]

8. Exchange rates

While a 1:1 ratio of metMbIm (or metMb4MeIm) and metMbH_2O mixture form readily by adding ~2 fold access of Im (or 4MeIm), ~ 20 fold access of 1MeIm is needed to form its 1:1 mixture to metMbH_2O. A large excess of 2-methylimidazole is required to achieve metMbH_2O : metMb(2MeIm) mixture, although free heme binds to 2MeIm readily in aqueous solution.[58] In some cases of hemoproteins,[59,60] with the influence of protein surroundings, the heme reactivities upon 2MeIm change. For metMb(2MeIm) the methyl group on the imidazole is too close to the heme plane, the steric hindrance likely lengthens the Im-Fe bond distance thus destablizes the complex.[59] In order to study the exchange rates of reaction 3, 6 and 7 quantitatively, 1D saturation transfer experiments at 50°C, pH 6.7 were performed for the following equine metMb complex mixtures in Figure 25-27: (a) metMbIm and metMbH_2O; (b) metMb1MeIm and metMbH_2O; (c) metMb4MeIm and metMbH_2O. Selective irradiation of the 5-methyl heme protons of the imidazole metMbs in each mixture giving saturation transfer to 5-methyl heme protons of metMbH_2O in the mixtures. To alleviate the problem of strong off-resonance effects from using high rf power, low

power (40 dB with irradiation time of 200 ms) irradiation was used. The lower spectra are from the irradiation, the middle spectra are the corresponding reference, the upper spectra are the difference between the reference and the corresponding irradiation spectra. Saturation factors were calculated using Equation 11 with correction for the incomplete irradiation. The spin lattice relaxation times of $5CH_3$ of $metMbH_2O$ at 323K is 5 msec, which is used to calculate the exchange rates k_{-1} using Equation 10. The results are tabulated in Table III.

The exchange rate constants of the exchange reactions at 323 K for water with metMbIm, metMb(1MeIm) and metMb(4MeIm) are 50, 127, 5.5 s^{-1} respectively. The extra methyl group allows 4MeIm likely fills the heme pocket more effectively. The more hydrophobic nature of the ligand stablizes the metMb(4MeIm) complex, which accounts for the much smaller exchange rate of reaction 5 than that of reaction 3. The exchange rate of reaction 4 is larger than that of reaction 3, sugguesting metMb(4MeIm) is less stable. Although 1MeIm and 4MeIm are similar in size and shape, they bind to metmyoglobin in a different fashion. Figure 28 illustrates that 4MeIm forms a hydrogen bond with its N_1H to the distal histidine 64 residue (Hs E7), as does Im in metMbIm, whereas 1MeIm does not have the ability to form this hydrogen bond. Thus a less stable complex and a faster off-rate k_{-1}.

Although the heme protons and heme pocket residues of metMbCN are fully assigned, this protein complex does not exchange its ligands with water at a sufficient rate to gain 2D EXSY cross-peaks, even at 323K (higher temperature causes rapid

denaturing of the protein). Therefore, obtaining the assignments of metMbH_2O through exchange metMbCN with water is impossible to realize. The irreversibility of this reaction is attributable to the strong interactions between the ligand CN^- and the iron.

CHAPTER IV

CONCLUSIONS

The study demonstrates the feasibility of 2D EXSY experiments to make assignments of many heme protons of metMbIm, metMb1MeIm, metMb4MeIm, metMbOH, and metMbSCN; additional assignment of $2H\beta_c$ and γ *meso* protons of $metMbH_2O$ are made. An alternative to isotopic labeling approach to gain heme proton assignments is established. In comparison to previous methods, which have yielded only the heme methyl resonance assignments of metMbIm, metMbOH, and metMbSCN, this new method gives assignments for each complex from a single 2D EXSY spectrum. The quantitative comparison of the linewidth of these complexes correlate with their high spin contents except for metMbIm. This abnormally broad linewidth of metMbIm has been suggested to the rotation of the imidazole ring around its pseudo C_2 axis. The study also demonstrates that saturation-transfer NMR can monitor directly the ligand binding kinetics in the myoglobin complexes. The difference in exchange rates of the imidazolate myoglobins are accounted for by the difference in hydrophilicity and ligand coordinating strength. These results will provide different opportunities to explore the structural and electronic mechanisms that influence ligand binding in myoglobin. In addition, this study provides a promising prelude for obtaining assignments for resonances of residues that reside

close in space to the paramagnetic iron of metMbH_2O via their EXSY cross peaks to the corresponding resonances of metMbIm, which can be obtainable using the conventional 2D NMR techniques.

REFERENCES

1. Voet, D and Voet, J.G. (1990) in Biochemistry, John Wiley & Sons, Inc, pp 210-216.
2. Mathews, C.K. and van Holde, K.E. (1990) in Biochemistry, the Benjamin/Cummings Publishing Company, Inc, pp133-135.
3. Rajarathnam, K., Qin, J., La Mar, G.N., Chiu, M.L., and Sligar, S.G., (1993) Biochemistry, 32, 5670-5680.
4. Allocatelli, C.T., Cutruzzola, F., Brancaccio, A., Brunori, M, Qin, J., and La Mar, G.N.(1993) Biochemistry, 32, 6041-6049.
5. Qin, J., La Mar, G.N., Dou, Y., Admiraal, S.J., and Ikeda-Saito, M., (1994) J. Biol. Chem., 269, 1083-1090.
6. Satterlee, J.D. (1986) Annu. Rep. N.M.R. Spectrosc., 17, 77-178.
7. Goff, H.M. (1983) in Iron Porphyrins (Lever, A.B.P. and Gray, H.B., eds), Addison-Wesley, Reading, Mass., 1983, Part 1, pp 239-281.
8. Mirtra, S. (1983) in Iron Porphyrins (Lever, A.B.P. and Gray, H.B., eds), Addision-Wesley, Reading, Mass., Part 2, pp. 1-42.
9. Palmer, G., (1983) in Iron Porphyrins ((Lever, A.B.P. and Gray, H.B., eds), Addision-Wesley, Reading, Mass., 1983, Part 2, pp. 43-88.
10. La Mar, G.N. (1979) in Biological Applications of Magnetic Resonance (Shulman, R.G., ed.), Academic Press, New York, 1979, pp. 305-343.

11. Morow, J.S. and Gurd, F.R.N. (1979) CRC Criti. Rev. Biochem., 3, 221-287.

12. Shulman, R.G., Glarum, S.H., and Karplus, M.(1971) J. Mol. Biol. 57, 93-115.

13. La Mar, G.N. and Walker, F.A. in The Porphyrins (Dolphin, D., ed.) Academic Press, New York, Vol. 4B, pp. 61-152.

14. Jesson, J.P. (1973) in NMR of Paramagnetic Molecules (La Mar, G.N., Horrocks, W.DeW, Jr. and Holm, R.H., eds.) Academic Press, New York, pp. 1-53.

15. Morrishima, I., Ogawa, S., Inubishi, T. & Iizuka, T. (1978) Adv. Biophys., 11, 217-245.

16. La Mar, G.N., Davis, N.L., Johson, R.D., Smith, W.S., Hauksson, T.B., Budd, D.L., Dalichow, F., Langry, K.C., Morris, I.K., and Smith, K.M. (1993) J. Am. Chem. Soc. 115, 3869-3876.

17. Smith, K.M. (1975) in Porphyrins and Metalloporphyrins (Smith, K.M.,ed.), Elsevier/North Holland Biomedial Press, Amsterdam, pp. 29.

18. Fuhrop, J.H. and Smith, K.M. (1975) in Porphyrins and Metalloporphyrins (Smith, K.M.,ed.), Elsevier/North Holland Biomedial Press, Amsterdam, pp. 757.

19. Smith, K.M. (1979) Accounts Chem. Res. 12, 374.

20. Smith, K.M., Fujinari, E.M., Langry, K.C., Parish, D.W. and Tabba, H.D. (1983) J. Am. Chem. Soc. 105, 6638.

21. Wüthrich, K., Shulman, R.G. and Peisach, J. (1968) Proc. Nat. Acad. Sci. USA, 60, 373.

22. Wüthrich, K., Shulman, R.G., Wyluda, B. and Caughey, W.S. (1968) Proc. Nat. Acad. Sci. USA. 62, 636.

23. La Mar, G.N., Budd, D.L., Sick, H. and Gersonde, K. (1978) Biochim. Biophys. Acta, 537, 270-283.

24. Latos-Grazynski, L., Balch, A.L. and La Mar, G.N. (1982) Adv. Chem. Ser., 201, 661.

25. Ramaprasad, S., Johnson, R.D., and La Mar, G.N. (1984) J. Am. Chem. Soc., 106, 3632.

26. Ramaprasad, S., Johnson, R.D., and La Mar, G.N. (1984) J. Am. Chem. Soc., 106, 5330.

27. Unger, S.W., Lecomte, J.T.J., and La Mar, G.N. (1985) J. Magn. Reson. 64, 521-528.

28. Bencini, A., Gatteschi, D., and Zanchini, C. (1980) J. Am. Chem. Soc. 102, 5234.

29. Kumar, A., Ernst, R.R and Wüthrich, K. (1980), Biochem. Biophys. Res. Commun. 95, 1-6.

30. Bax, A., Freeman, R. and Morris, G. (1981) J. Magn. Reson. 42, 164-168.

31. Marion, D. & Wüthrich, K. (1983) Biochem. Biophys. Res. Commun. 113, 967-974.

32. Wüthrich, K. (1986) in NMR of Proteins and Nucleic Acids., Wiley, New York.

33. Emerson, S.D & La Mar, G.N. Biochem.(1990), 29, 1545-1556.

34. Yu, L, La Mar, G.N., and Rajarathnam, K. (1990) J. Am. Chem. Soc. 112, 9527-9534.

35. Wand, A.J., Di Stefano, D.L., Feng, Y., Roder, H., and Englander, S.W. (1989) Biochemistry, 28, 186-194.

36. Peyton, D.H. (1990) Biochem. Biophys. Res. Commun. 175(2), 515-519.

37. Jeener, J., Meier, B.H., Bachmann, P., and Ernst, R.R. (1979) J. Chem. Phys., 71, 4546-4553.

38. Macura, S., Westler, W.M. and Markley, J.L. (1994) Methods in Enzymology, 239,106-144.

39. Meier, B.H. and Ernst, R.R. (1979) J. Am. Chem. Soc. 101, 6441-6442.

40. Yee, S. (1993) Solution-State Proton Nuclear Magnetic Resonance (NMR) Spectroscopic Studies of the Active Sites of Myoglobins in Various Ligated State as Models for Macromolecule-Substrate Binding and Advancement of Paramagnetic NMR Techniques, Ph.D Dissertation.

41. La Mar, G.N., Budd, D.L. and Smith, K.M. (1980) Biochim. Biophys. Acta, 622, 210-218.

42. La Mar, G.N., Budd, D.L. Smith, K.M. & Langry, K.C. (1980) J. Am. Chem. Soc. 102(6), 1822-1827.

43. Yamamoto, Y. (1993) Biochem. Biophys. Res. Commun., 196, 348-354.

44. Bertini, I. and Luchinat, C. (1986) in NMR of Paramagnetic Molecules in Biological Systems, the Benjamin/Cummings Publishing Co., Inc.

45. Marion, D. & Wüthrich, K. (1980) Biochem. Biophys. Res. Commun. 95, 1-6.

46. Rance, M., Sorenawn, O.W., Bodenhausen, G., Wagner, G., Ernst, R. R. and Wüthrich, K.(1983) Biochem. Biophys. Res. Commun., 117, 479-485.

47. La Mar, G.N. (1973) in NMR of Paramagnetic Molecules, (La Mar, G. N., Horrocks, W. D., Jr. and Holm, R. H., Eds.) pp. 86-157, Academic Press, New York.

48. Harris, R.K. (1983) in Nuclear Magnetic Resonance Spectroscopy, A Physicochemical View, Longman Scientific & Technical, England.

49. Algar, J. and Shulman, R.G. (1983) Q. Rev. Phys. 17, 83-124.

50. Sandström, J. (1982) in Dynamic NMR spectroscopy, Academic press.

51. Caughey, W.S (1966) in Hemes and Hemoproteins (Chance, B., Estabrook, R.W. a and Yohetani, T., Eds.) pp 276-277, Academic Press, New York.

52. McGrath, T.M. and La Mar, G.N. (1978) Biochim. Biophys. Acta, 534, 99-111.

53. Iizuka, T. and Kotani, M. (1968) Biochim. Biophys. Acta 154, 417-419.

54. Antonini, E. and Brunori, M. (1971) in Hemoglobin and Myoglobin in Their Reactions with Ligands, North-Holland, Amsterdam.

55. Iizuka, T. and Kotani, M. (1969) Biochim. Biophys. Acta 181, 275-286.

56. Iizuka, T. and Morrishima, I. (1974) Biochim. Biophys. Acta 371, 1-13.

57. Qin, J., La Mar, G.N., Asoli, F., and Brunori, M. (1993) J. Mol. Biol., 231 (4), 1009- 1023.

58. Eaton, D.R., and Wilkins, R.G. (1978) J. Biol. Chem., 253, 908-915.

59. Decatur, S.M. and Boxer, S.G. (1995) Biochemistry, 34, 2122-2129.

60. 2-methylimidazole does not bind to heme oxygenase H32A mutant, private communication with Dr.Thomas M. Loehr from Oregon Graduate Institute.

TABLE I. ^{1}H NMR assignments of heme protons in equine metMbH_2O, metMbSCN, metMbOH and metMbIm at 323K

heme protons	metMbH_2O	metMbSCN	metMbOH	metMbIm
1CH3	50.9	46.2*	29.1	25.0
3CH3	70.0	53.3	37.5	7.5
5CH3	82.6	58.8	43.0	38.5
8CH3	89.0	63.5	43.8	17.6
$2H_\alpha$	44.7	34.2*	26.3*	23.2
$2H_{\beta c}$	-5.8*		1.8*	-1.6
$2H_{\beta t}$	-6.4			-3.0
$4H_\alpha$	31.8	32.4*	21.5*	8.3
$4H_{\beta c}$				-1.0*
$4H_{\beta t}$				-1.3*
$6H_\alpha$	54.4	47.8*	36.8*	15.4
$6H_\alpha$'	44.7	34.2*	25.9*	13.5
$6H_\beta$				2.5
$6H_\beta$'				2.3
$7H_\alpha$	67.4	10.8*	13.8*	6.8
$7H_\alpha$'	30.8		10.8*	2.6
$7H_\beta$	17.0		20.1*	2.5
$7H_\beta$'				
α-meso				9.6*
β-meso				7.42*
γ-meso	48*			11.0*
δ-meso				

* Assigned in this study, the rest of the assignments were obtained based on the reference 24, 28, 37.

TABLE II.

T_1 measurements (msec) of heme protons in equine metMbH_2O, metMbSCN, metMbOH,metMbIm, metMb(1MeIm) and metMb(4MeIm) at 323 K.

heme protons	metMbH_2O	metMbSCN	metMbOH	metMbIm
1CH3	1.0	4.6	2.1	31.4
3CH3	4.1	4.9	2.0	
5CH3	5.0	4.7		33.7
8CH3	5.2	5.0	1.7	40.1
$2H_\alpha$		3.6	1.54	30.2
$2H_{\beta c}$				
$2H_{\beta t}$				
$4H_\alpha$	2.8	2.5	1.03	
$4H_{\beta c}$				
$4H_{\beta t}$				
$6H_\alpha$	5.5	5.9		33.5
$6H_\alpha$'	3.2			31.1
$6H_\beta$				
$6H_\beta$'				
$7H_\alpha$	18.6			
$7H_\alpha$'	14.8			
$7H_\beta$				
$7H_\beta$'				
α-meso				
β-meso				
γ-meso				
δ-meso				

TABLE II (continued)

T_1(msec) measurements of heme protons in equine metMb(1MeIm) and metMb(4MeIm) at 323K

heme protons	metMb(1MeIm)	metMb(4MeIm)
1CH3	26.6 msec	43.3 msec
3CH3		
5CH3	26.0	38.9
8CH3	28.8	20.0
$2H_{\alpha}$	33.3	32.9
$2H_{\beta c}$		
$2H_{\beta t}$		
$4H_{\alpha}$		
$4H_{\beta c}$		
$4H_{\beta t}$		
$6H_{\alpha}$	22.6	25.1
$6H_{\alpha}$'	26.3	22.8
$6H_{\beta}$		
$6H_{\beta}$'		
$7H_{\alpha}$		
$7H_{\alpha}$'		
$7H_{\beta}$		
$7H_{\beta}$'		
α-meso		
β-meso		
γ-meso		
δ-meso		

TABLE III Exchange rates and saturation factors (F) between metMbH_2O and metMbIm; methyl substituted imdidazole metmyoglobins at 323K based on 1D saturation transfer experiments

Reactions	3	4	5
Saturation factors	0.69	0.56	0.93
k_{-1} (s^{-1})	90	156	15

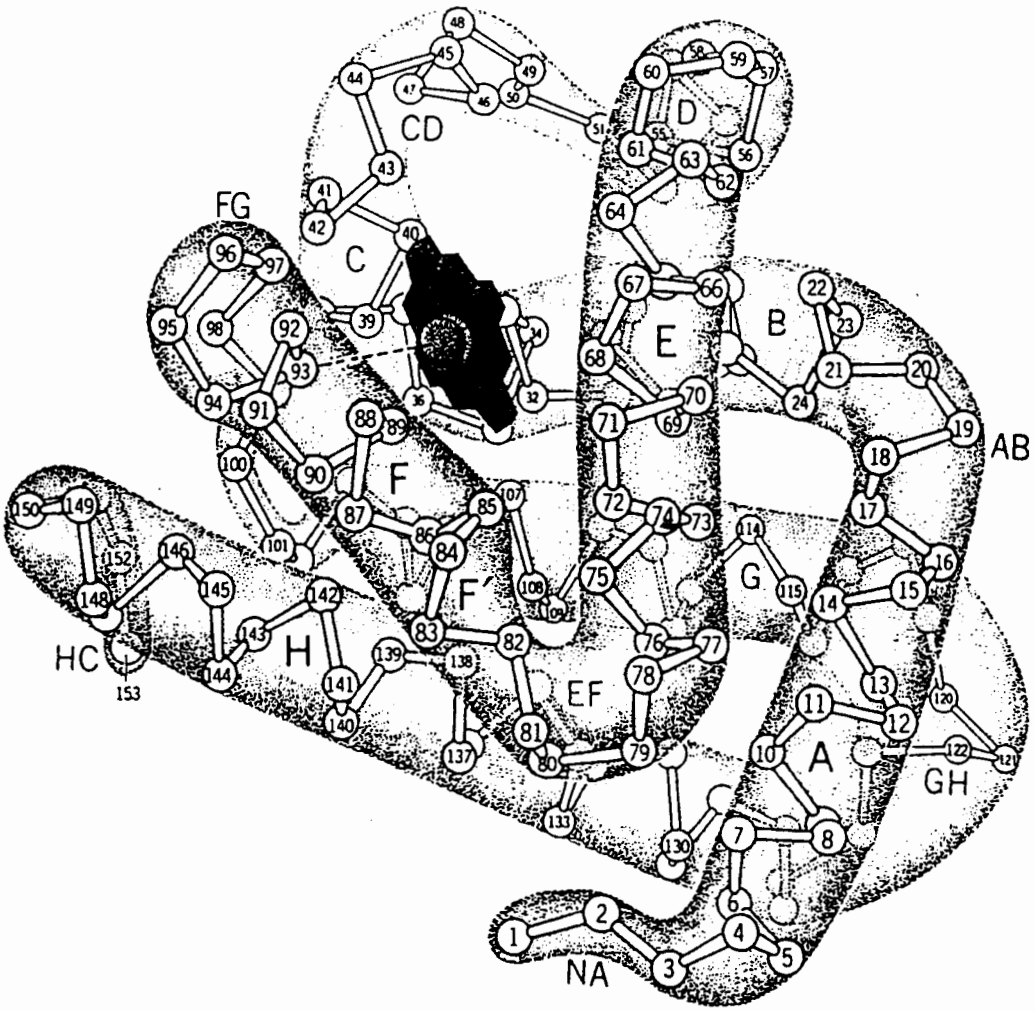

Figure 1. Three-dimensional crystal structure of sperm whale myoglobin.[2] Each amino acid is indicated by a circle corresponding to its a-carbon atom. Individual α-helical regions are labeled A-H, with turn regions designated by two letters, eg, EF.

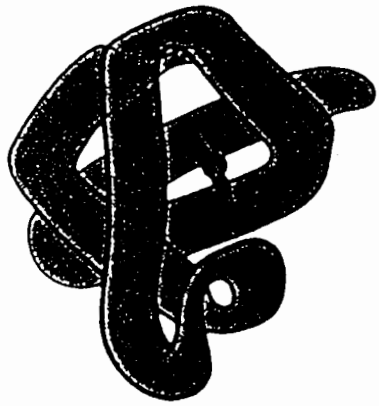

Myoglobin

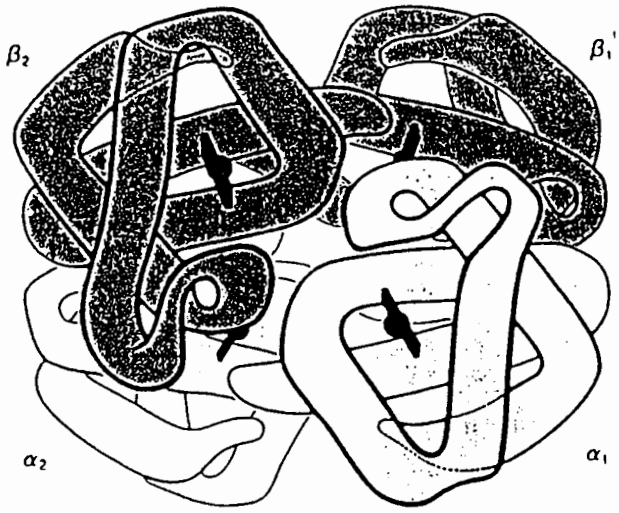

Hemoglobin

Figure 2. Comparison of myoglobin and hemoglobin structures.[2]

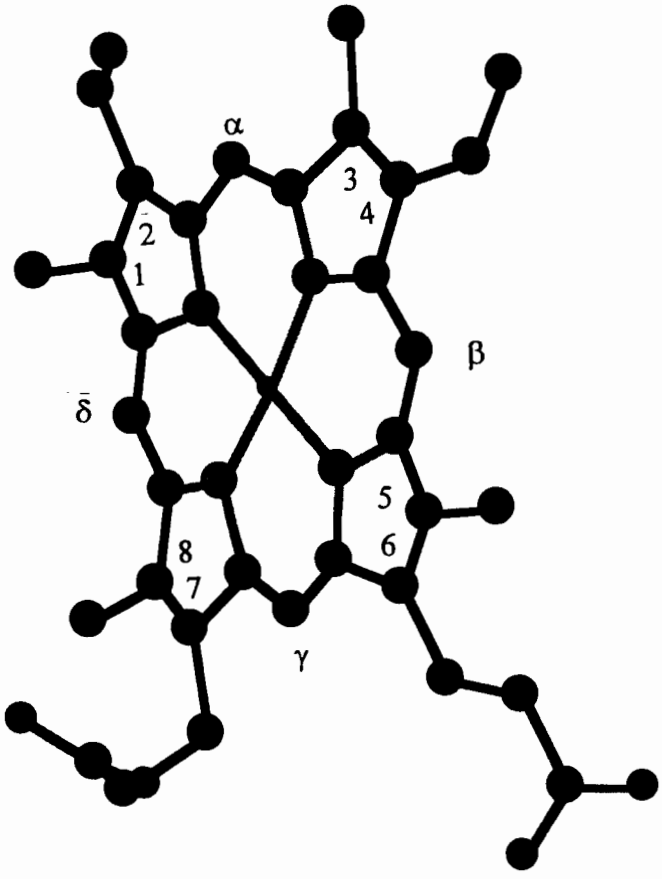

Figure 3. Structure of heme in myoglobin

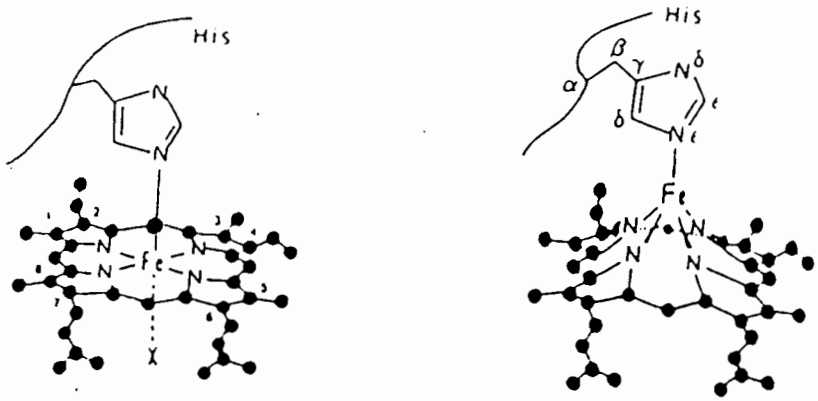

LOW SPIN

FE^{2+}: $X = O_2, CO$
OXYHB
OXYMB
HB-CO
MB-CO

FE^{3+}: $X = CN^-$
HB-CN
MB-CN
CCP-CN
HRP-CN

HIGH SPIN

FE^{2+}: DEOXY HB
DEOXY MB

FE^{3+}: METAQUO HB
METAQUO MB
PEROXIDASES

Figure 4. Ligation states in high-spin and low-spin myoglobin complexes.

Protein	Myoglobin (Mb) Hemoglobin (Hb)	Oxymyoglobin (MbO_2) Oxyhemoglobin (HbO_2) Ferrocytochrome-c	Metmyoglobin ($Mb \cdot H_2O$) Methemoglobin ($Hb \cdot H_2O$)	Cyanoferrimyoglobin (MbCN) Cyanoferrihemoglobin (HbCN) Ferricytochrome-c
Oxidation state	Fe(II)	Fe(II)	Fe(III)	Fe(III)
Spin state	$S = 2$	$S = 0$	$S = \frac{1}{2}$	$S = \frac{1}{2}$
Electron configuration				
$d_{x^2-y^2}$	↑	—	↑	—
d_{z^2}	↑	—	↑	—
d_{xy}	↑	↑↓	↑	↑
d_{xz}	↑	↑↓	↑	↑↓
d_{yz}	↑↓	↑↓	↑	↑↓

Figure 5. Electronic states in myoglobin complexes.

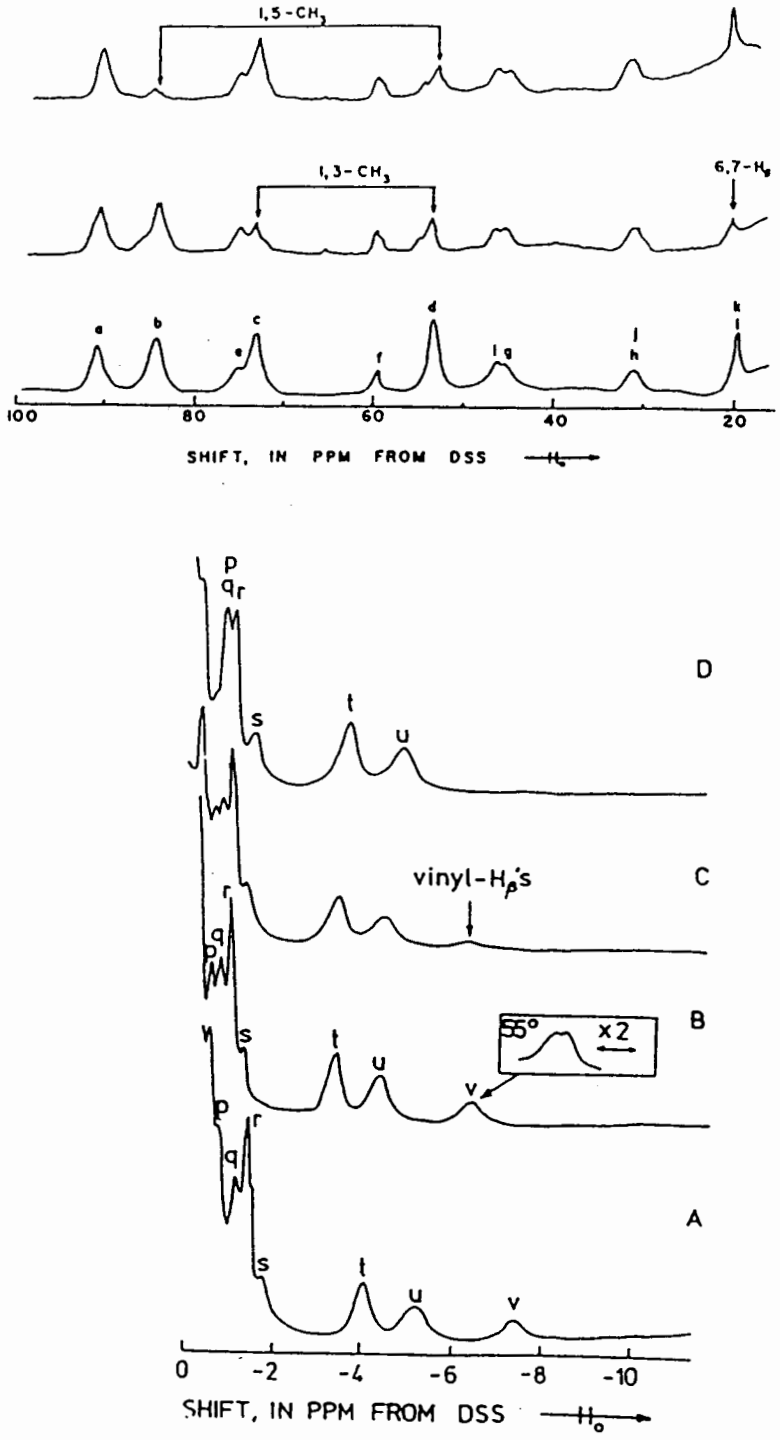

Figure 6. Assignment of methyl protons and vinyl protons by deuterium isotope labeling for metMbH_2O.[41]

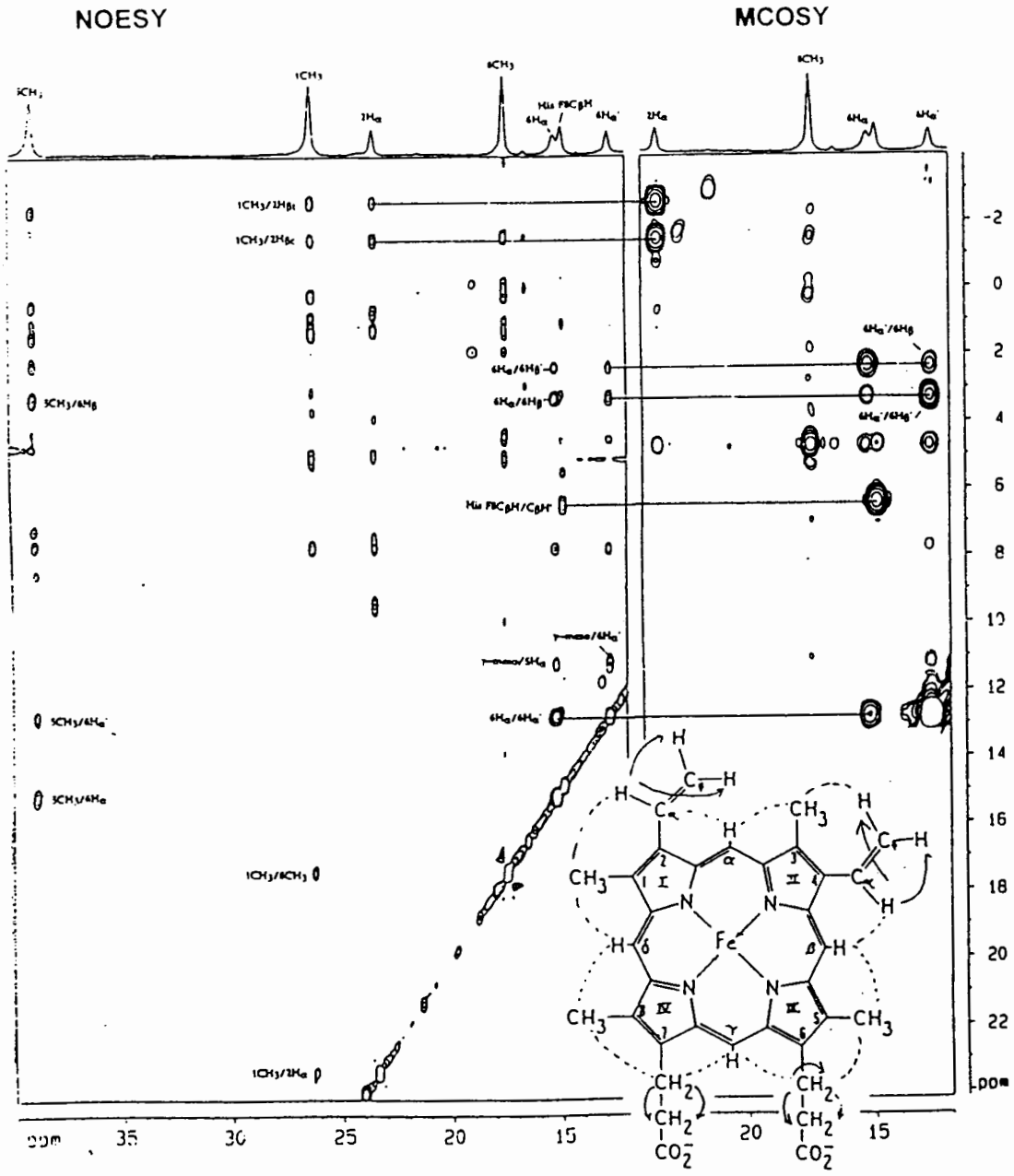

Figure 7. Assignment of heme protons by 2D NOESY/COSY experiments in metMbIm, pH 6.8, 304 K, according to previous work.[40] The correlations are indicated by the horizontal and vertical lines.

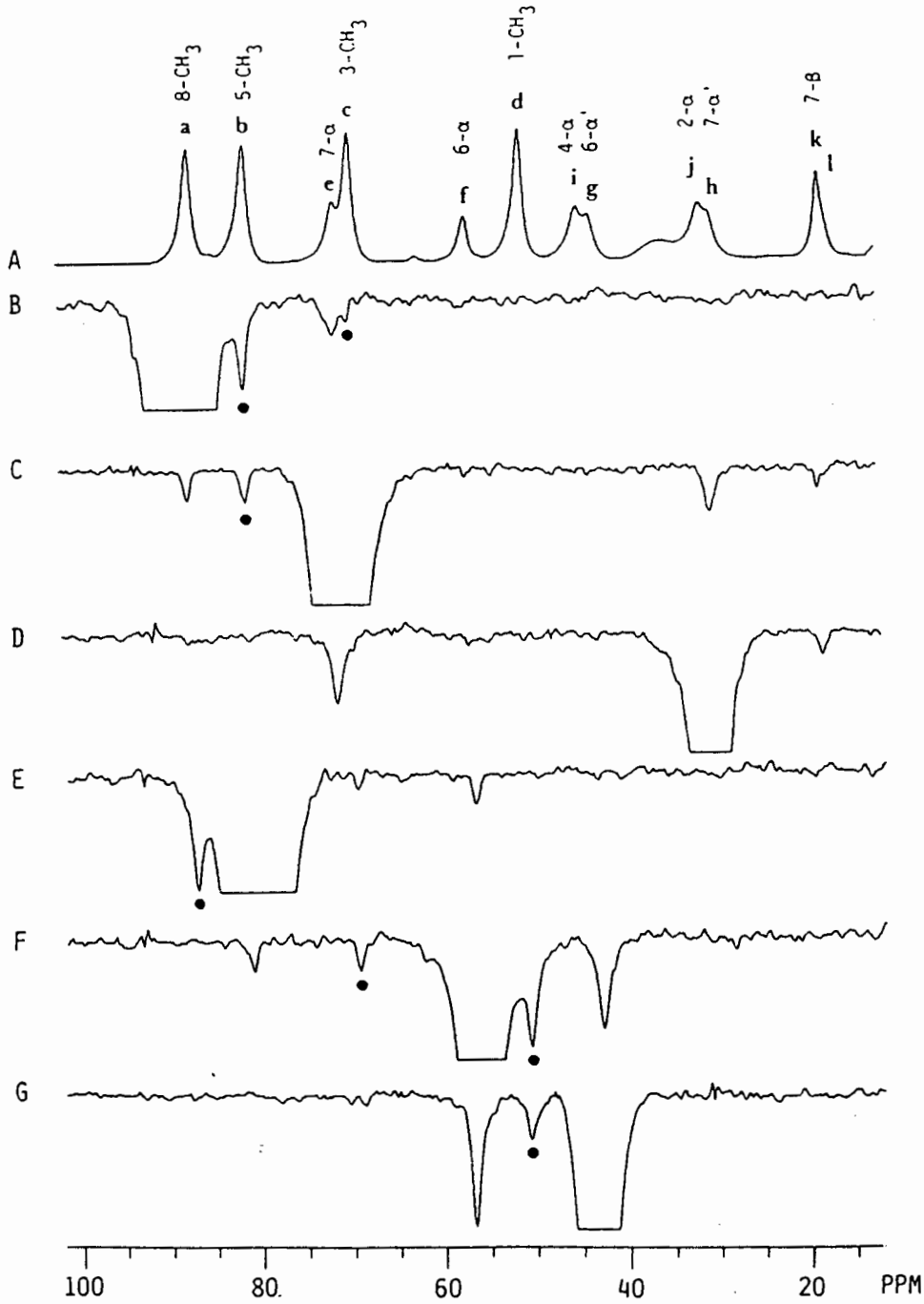

Figure 8. Assignment of heme protons by by 1D NOE in metMbH_2O, pH 6.4, 313 K.[27] The dots denote off-resonance effect upon irradiation.

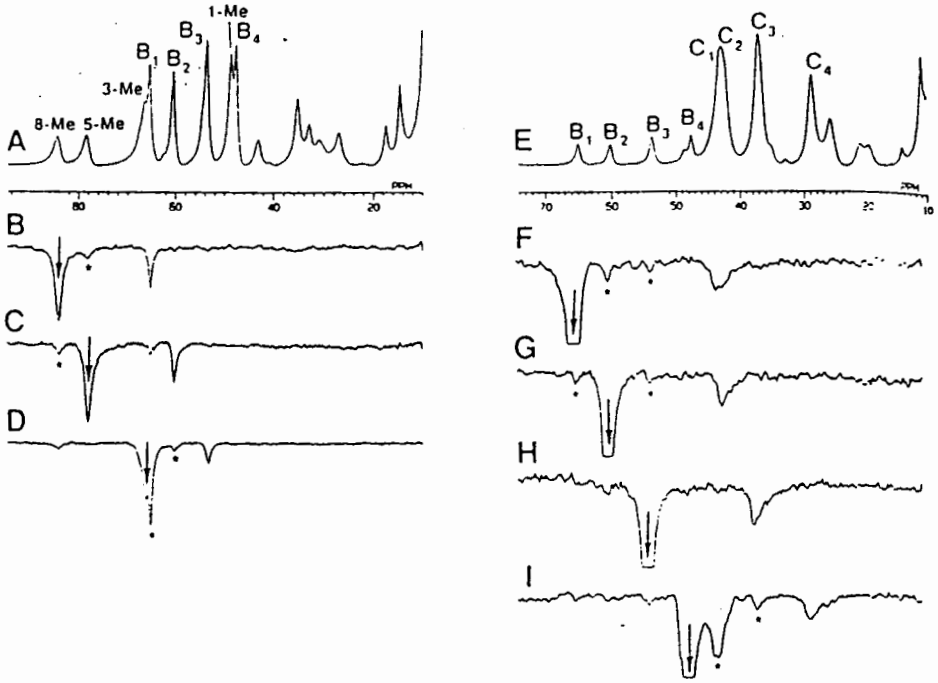

Figure 9. Assignment of methyl heme protons of equine metMbSCN and metMbOH by 1D saturation transfer.[43]

A. Reference spectrum of $metMbH_2O$ and metMbSCN at pH 7.32.

B-D. Irradiate 8, 5 and 3-methyl groups of $metMbH_2O$, respectively.

E. Reference spectrum of metMbOH and metMbSCN at pH 10.39.

F-I. Irradiate peak B1, B2, B3 and B4 of metMbSCN, respectively.

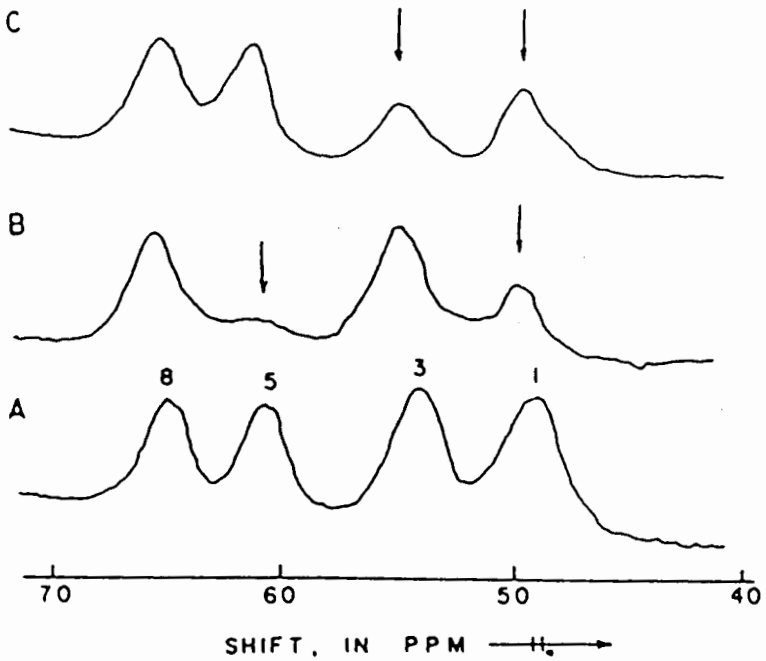

Figure 10. Downfield hyperfine region of the proton NMR spectra of metMbSCN at 298 K.[42] A. Reference spectrum. B. metMbSCN reconstituted with heme deuteriated at 1-methyl (~ 65%) and 5-methyl (90%) C. metMbSCN reconstituted with heme deutereiated at 1-methyl (40%) and 3-methyl (60%)

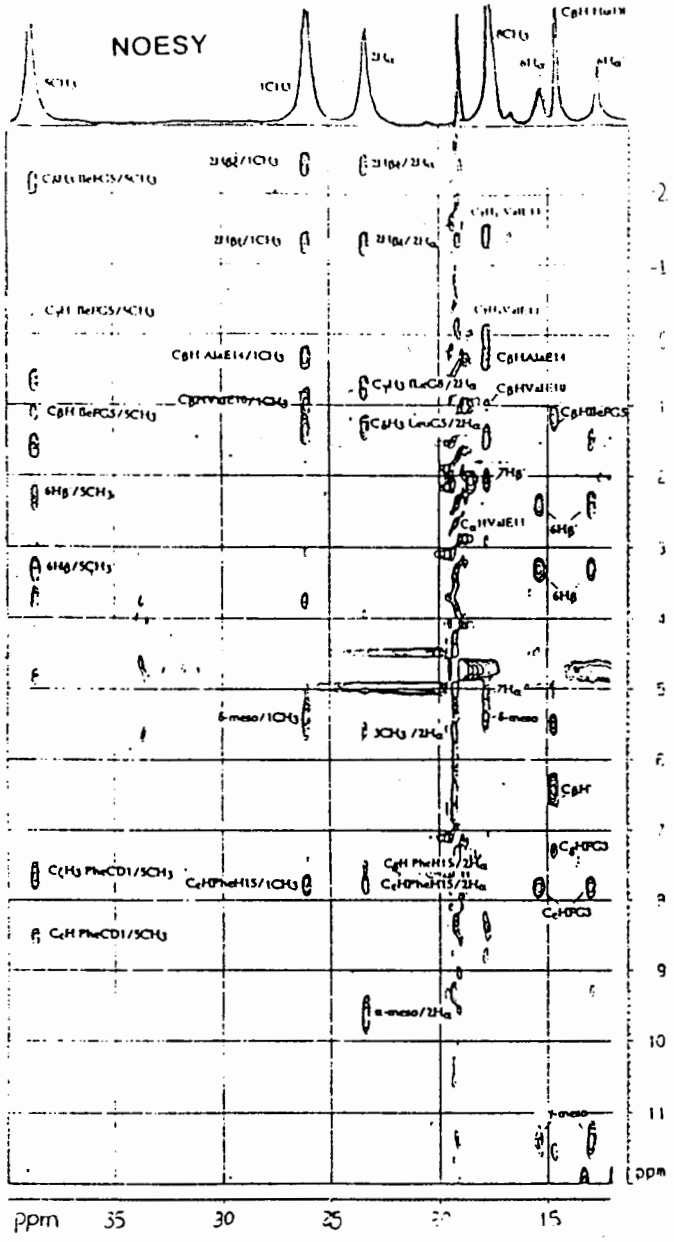

Figure 11. Additional assignment of heme protons of metMbIm by 2D NOESY/COSY/ TOCSY experiments.

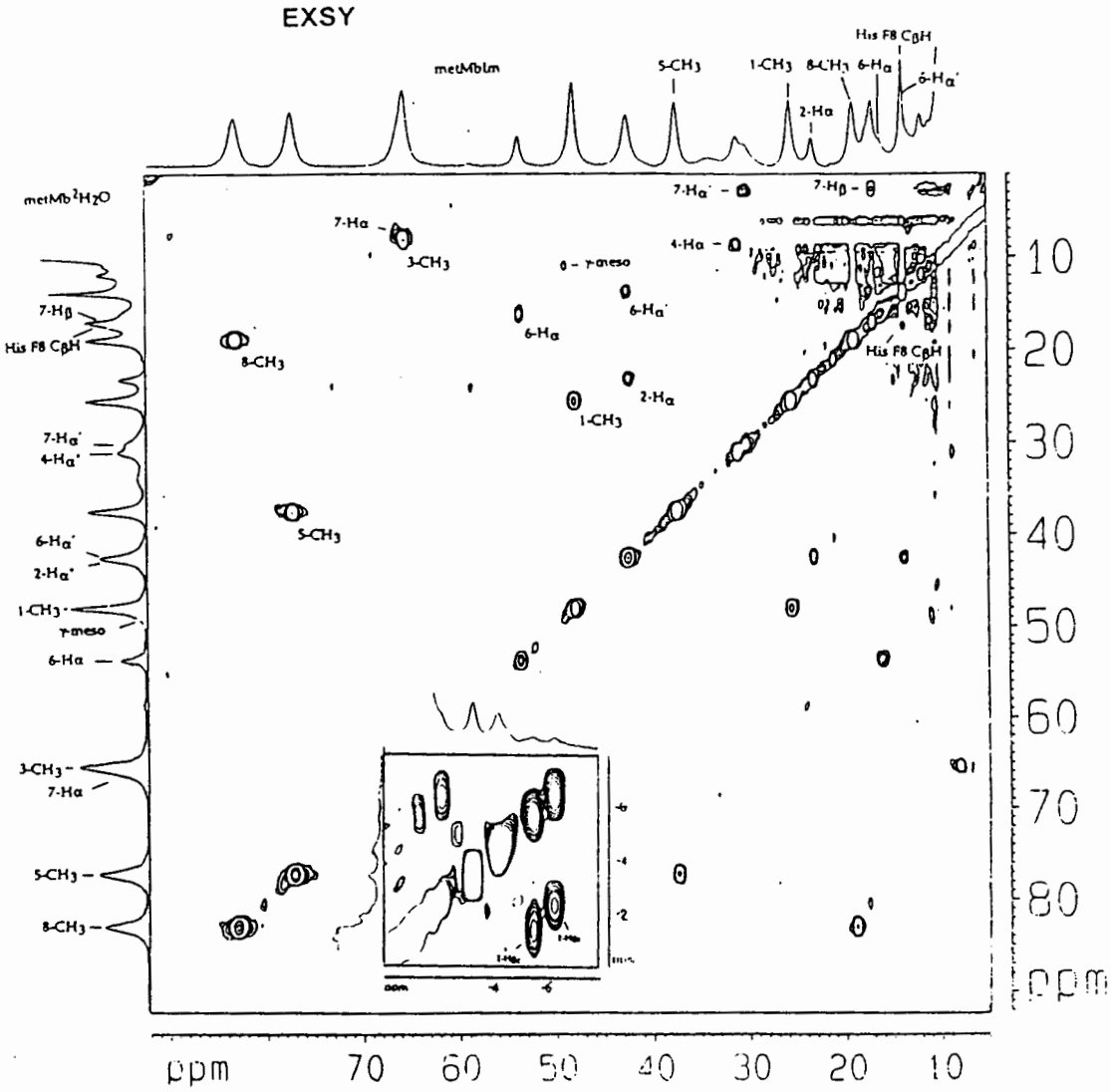

Figure 12. 2D EXSY spetrum of metMbIm / metMbH_2O mixture to gain extra assignments of metMbH_2O

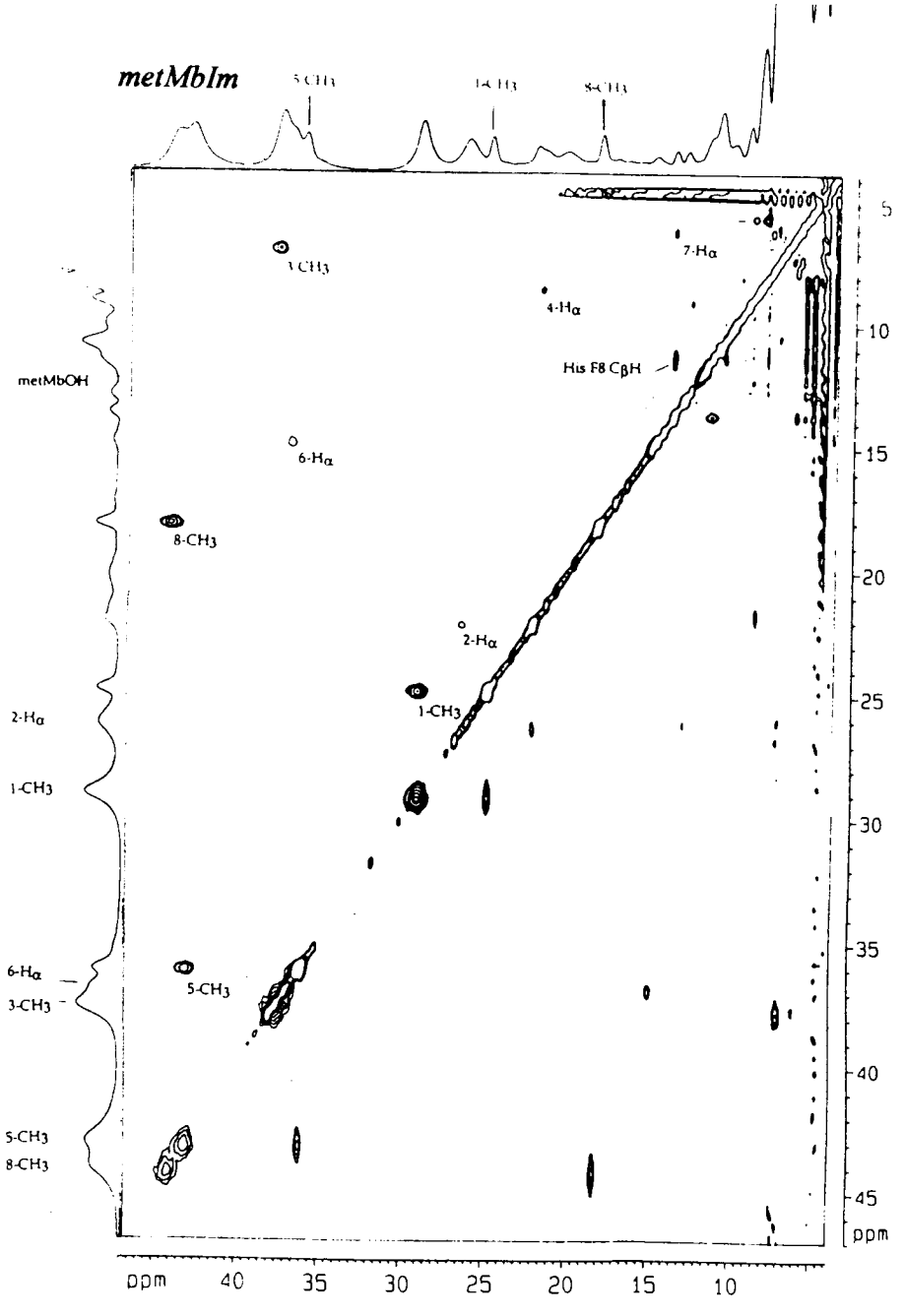

Figure 13. 2D EXSY spectrum of metMbIm / metMbOH mixture.

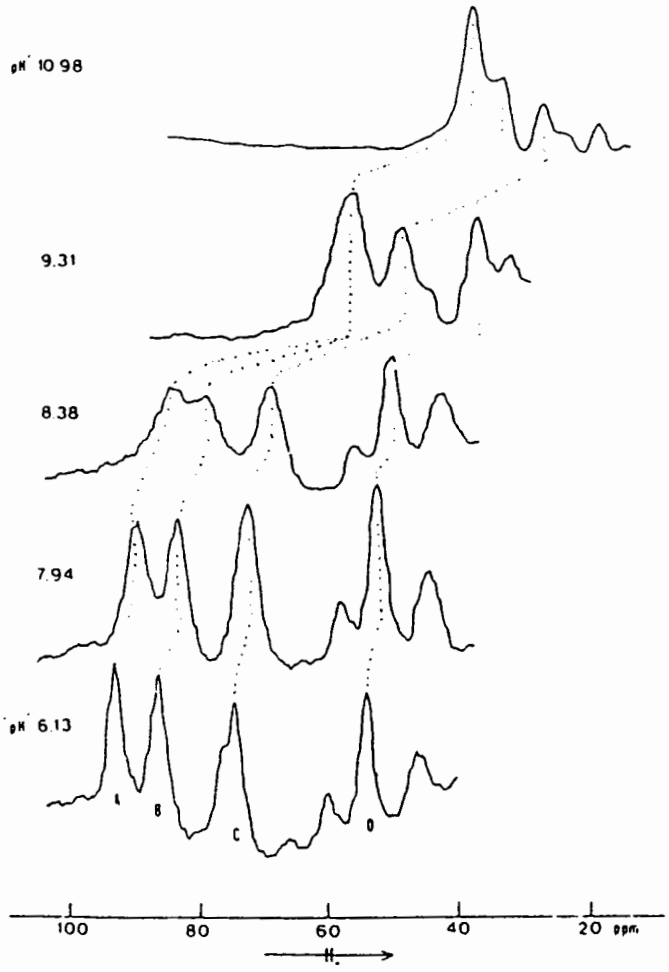

Figure 14. Acid to base transition of equine metmyoglobin .

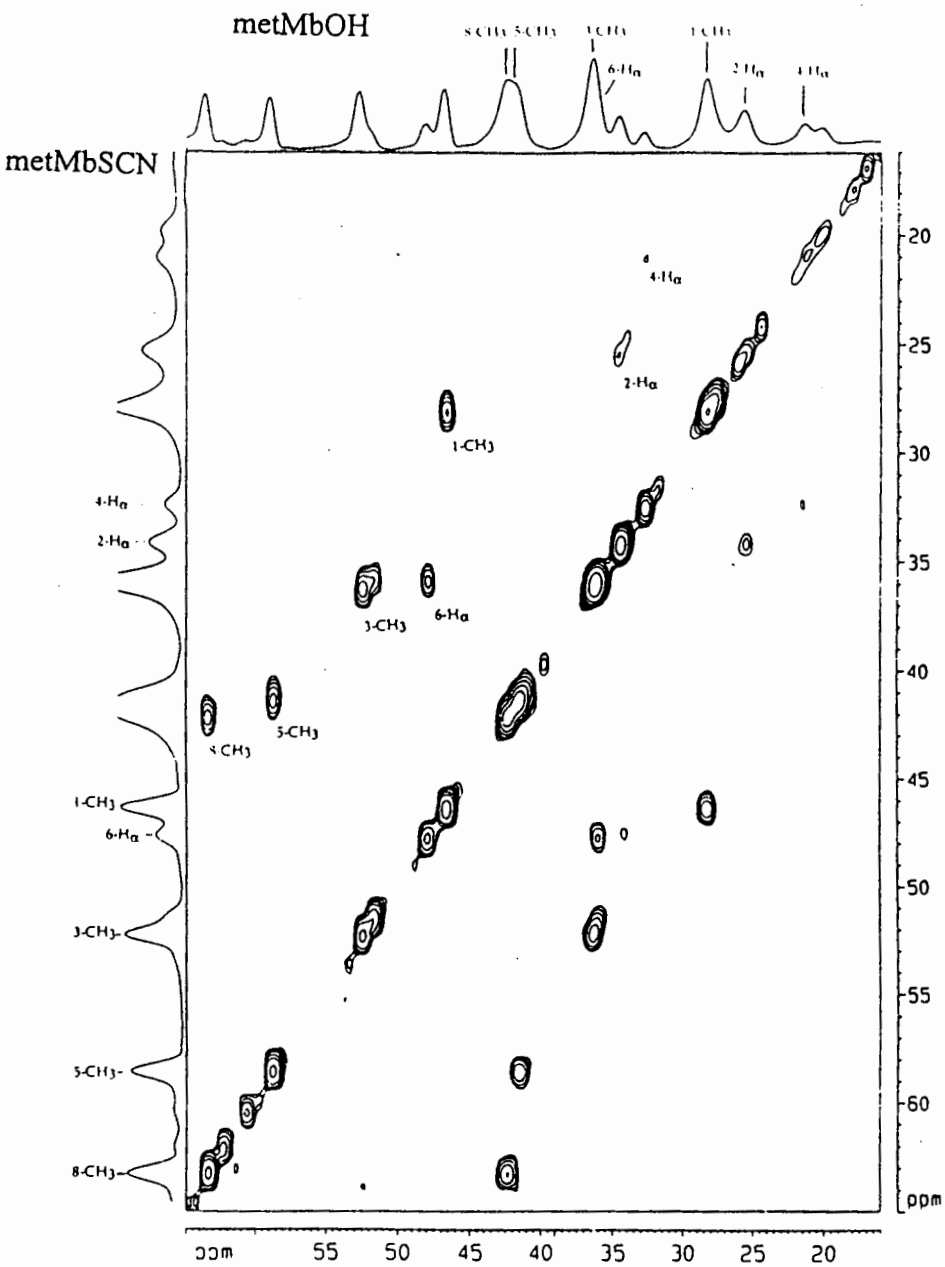

Figure 15. 2D EXSY spectrum of metMbOH / metMbSCN mixture.

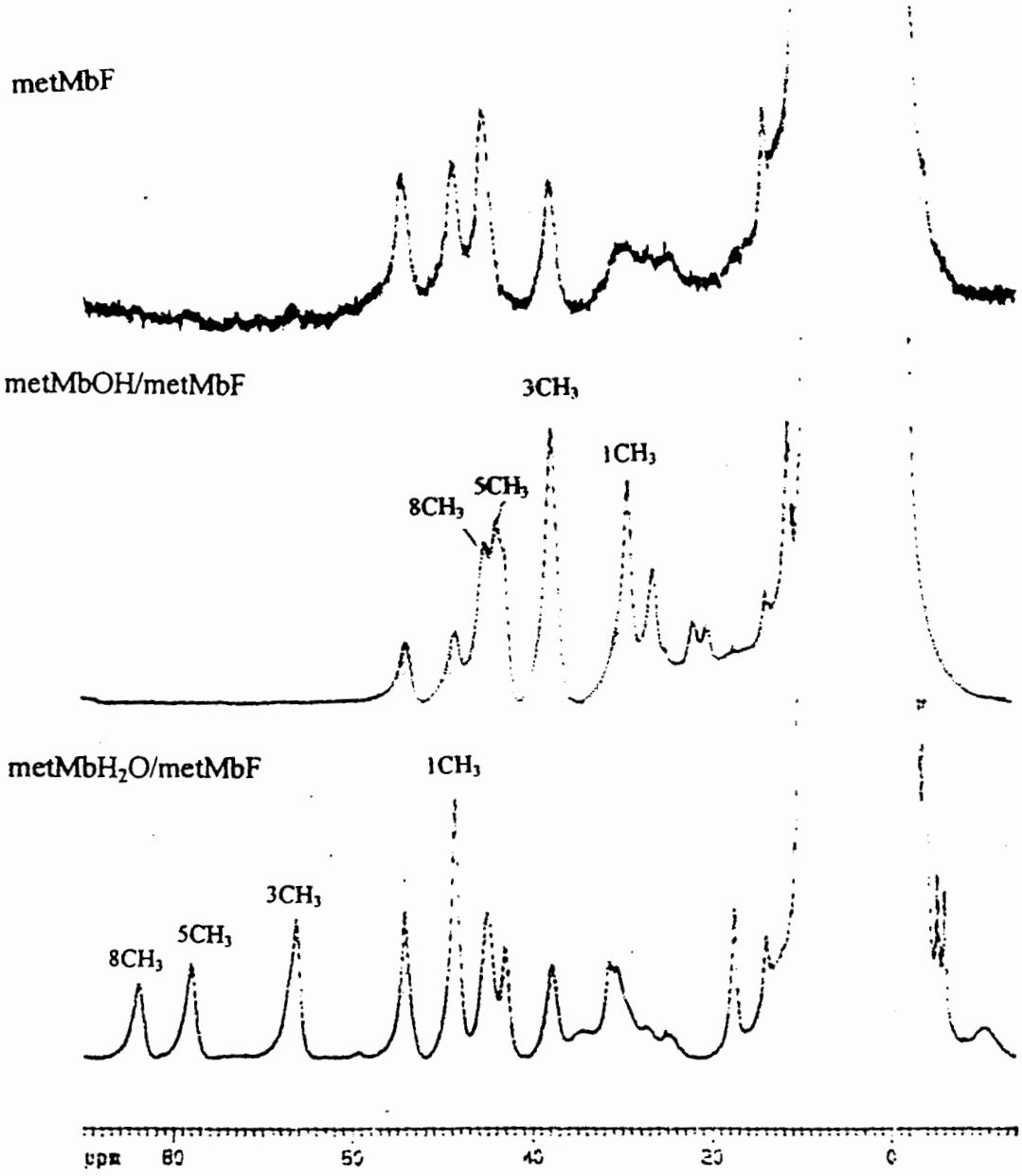

Figure 16. ^{1}H NMR spectrum of metMbH_2O/metMbF and metMbOH/metMbF mixtures.

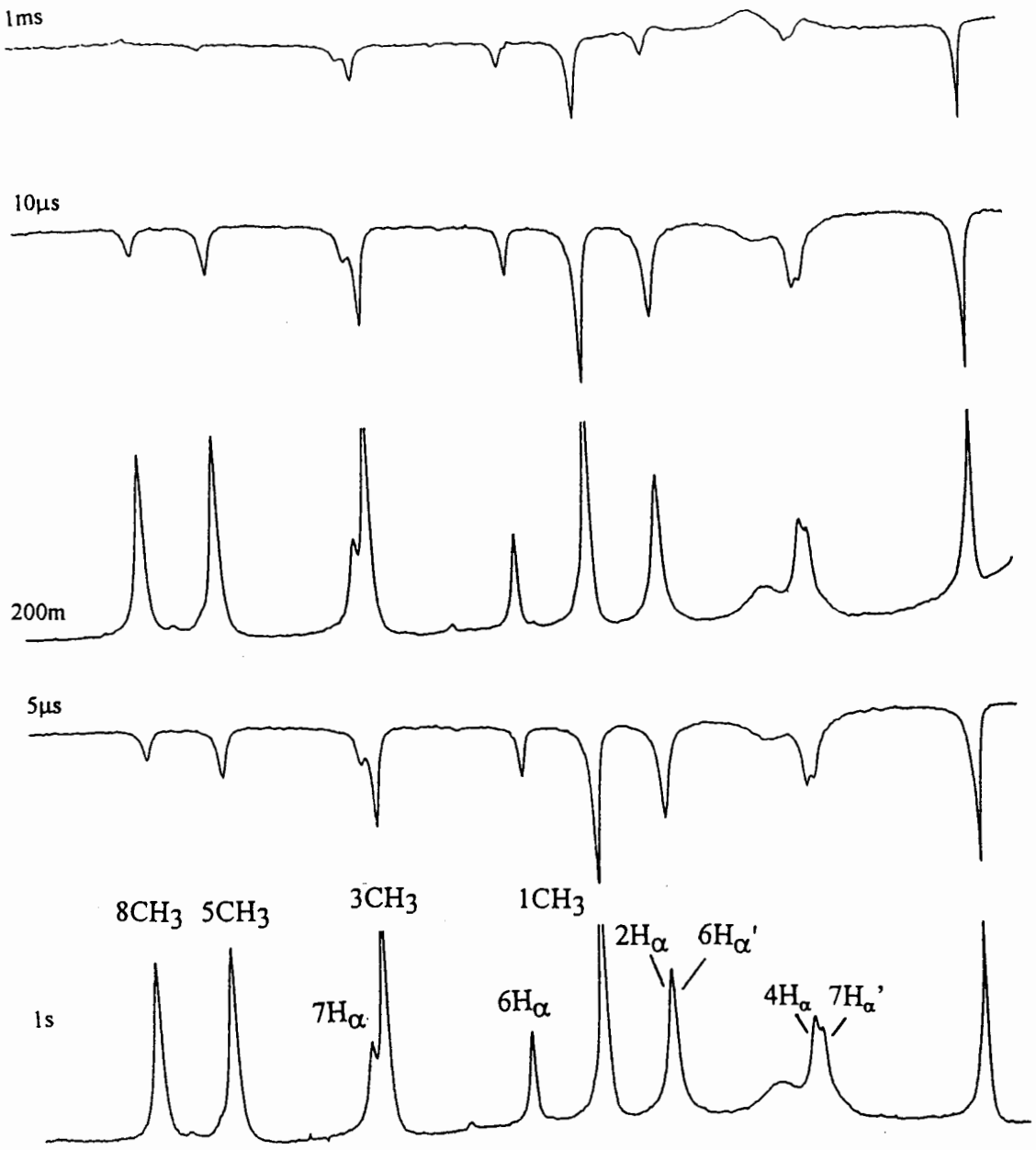

Figure 17. T_1 experiment of metMbH_2O at 323K.

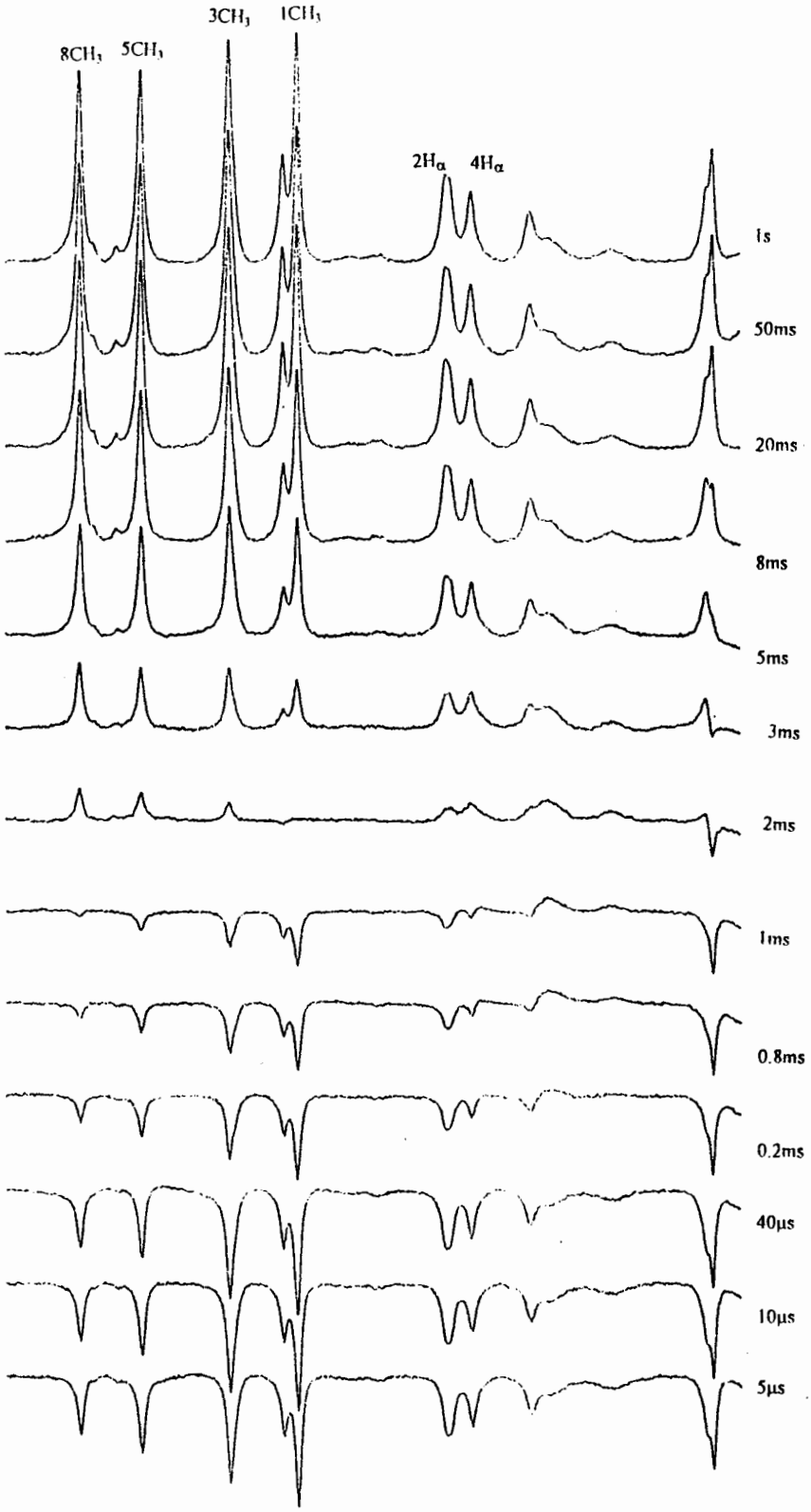

Figure 18. T_1 experiment of metMbSCN at 323K.

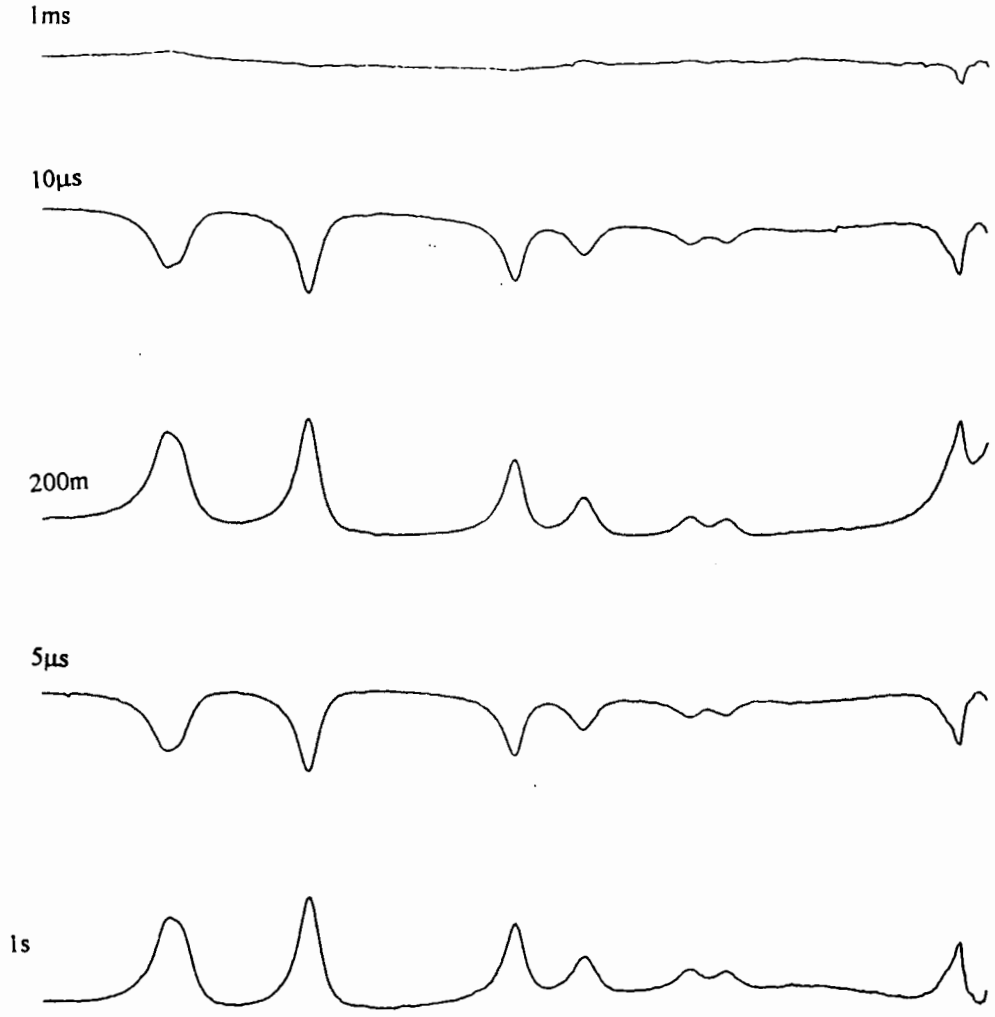

Figure 19. T_1 experiment of metMbOH at 323K.

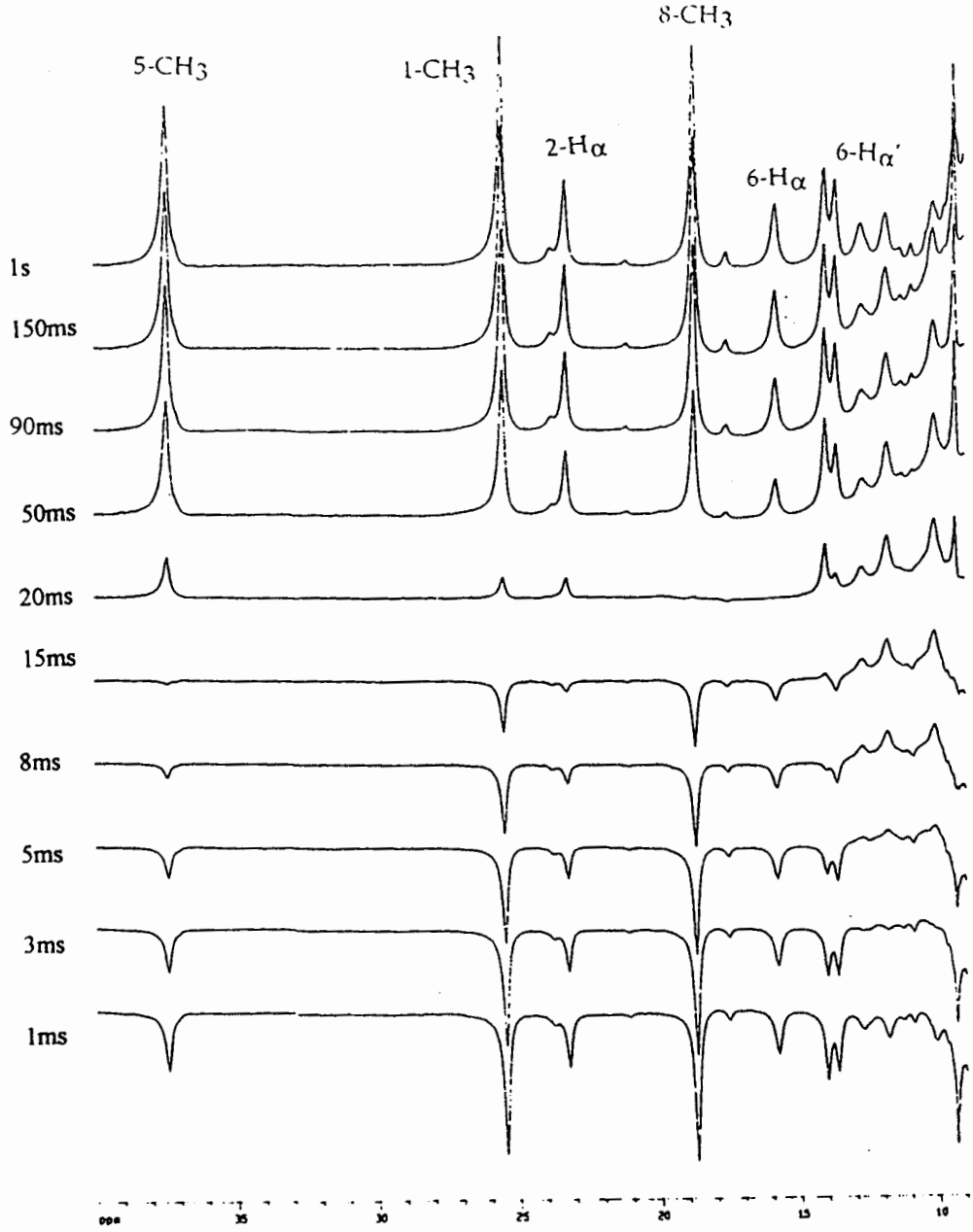

Figure 20. T_1 experiment of metMbIm at 323K.

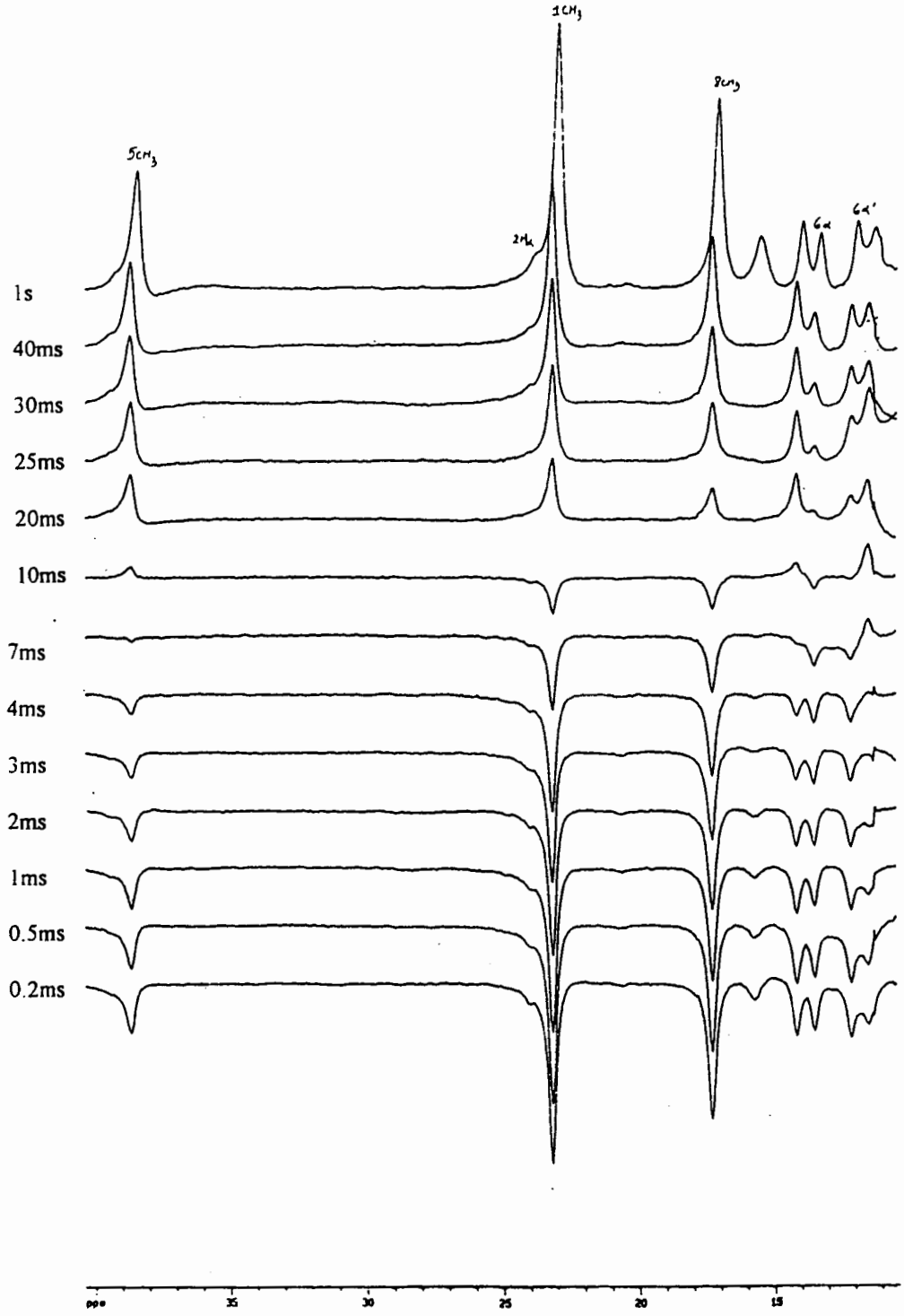

Figure 21. T_1 experiment of metMb(1MeIm) at 323K.

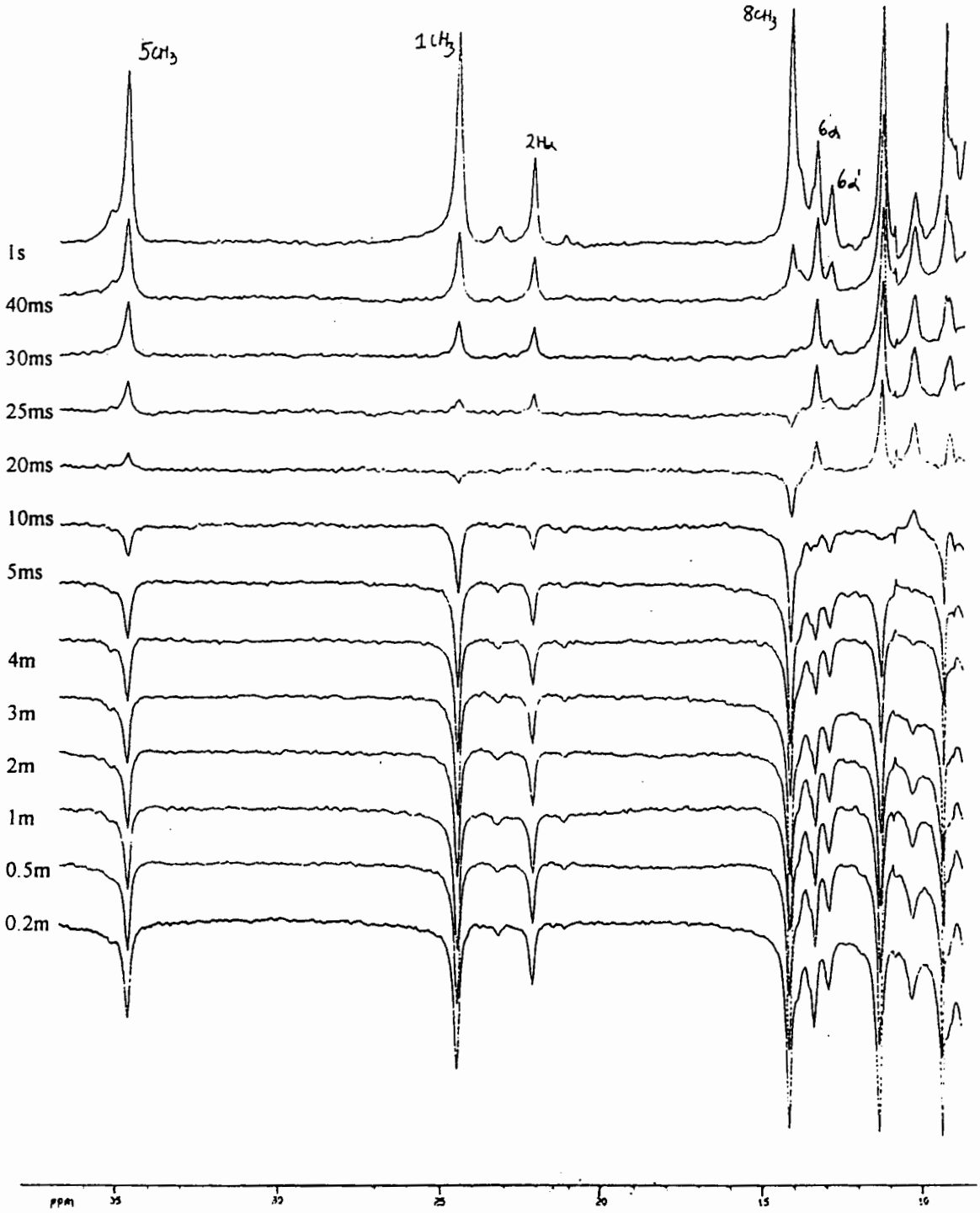

Figure 22. T_1 experiment of metMb(4MeIm) at 323K.

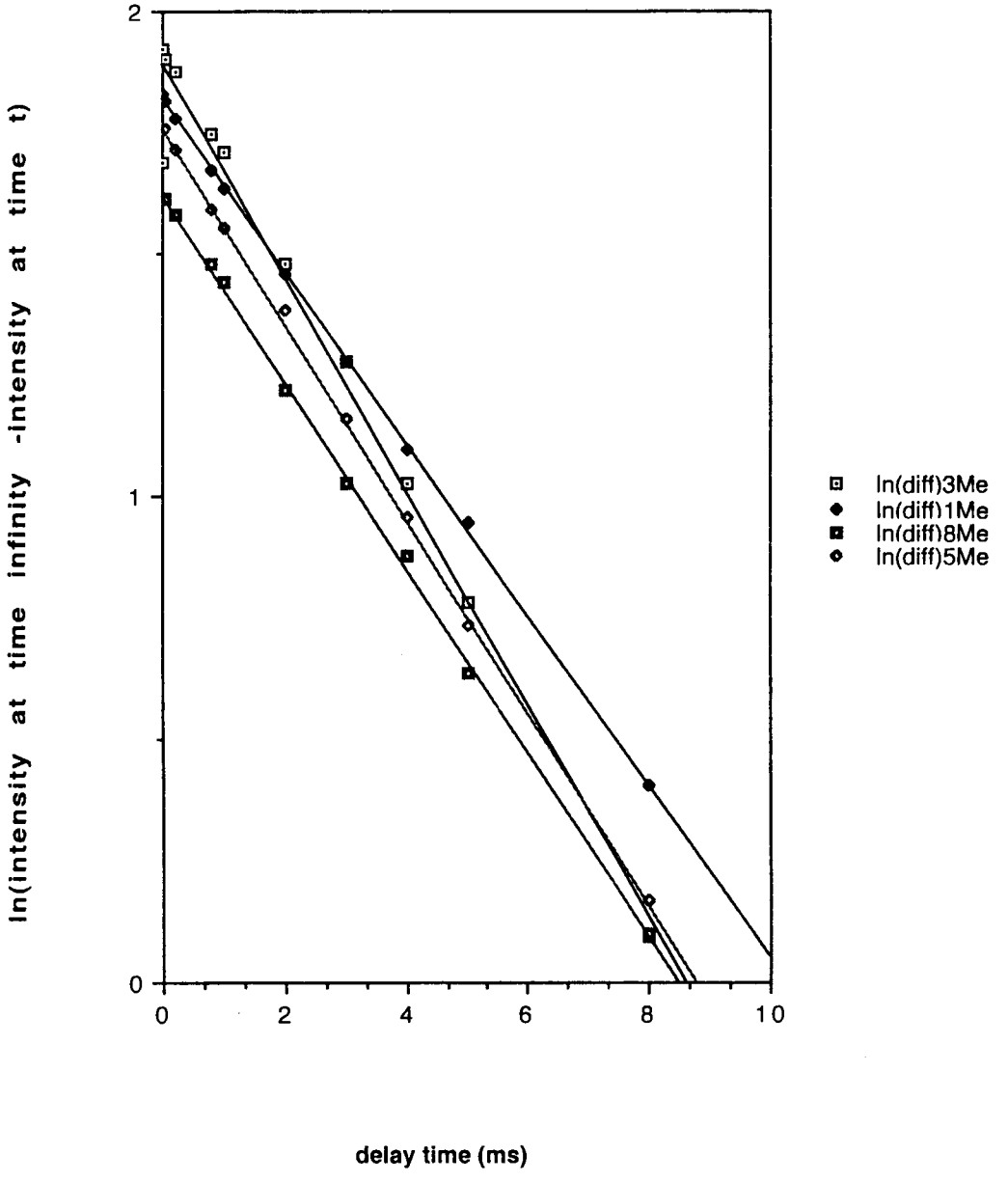

Figure 23. Examples of plots for T_1 determinations: methyl groups of $metMbH_2O$ at 323K.

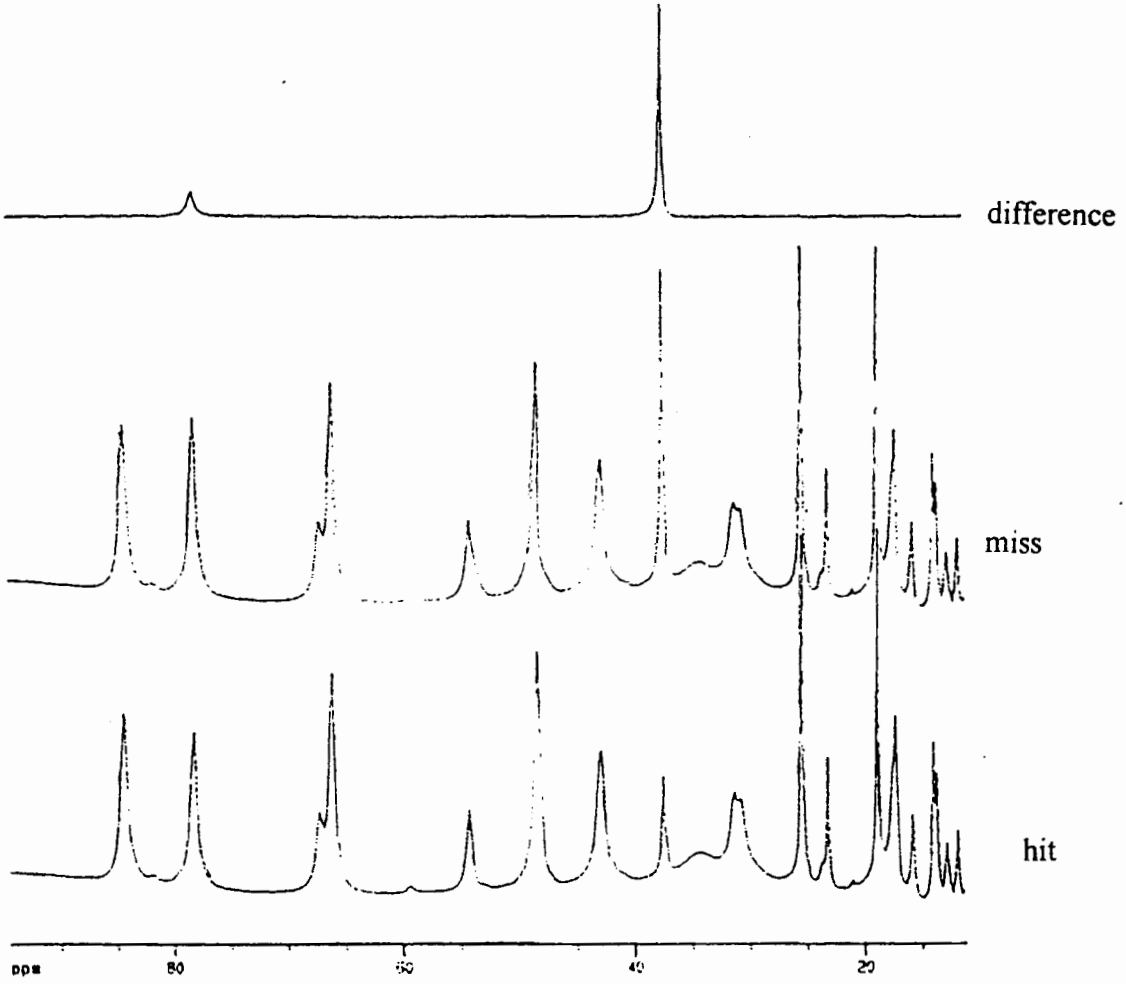

Figure 24. 1D saturation transfer experiment in metMbH_2O / metMbIm mixture at 323 K.

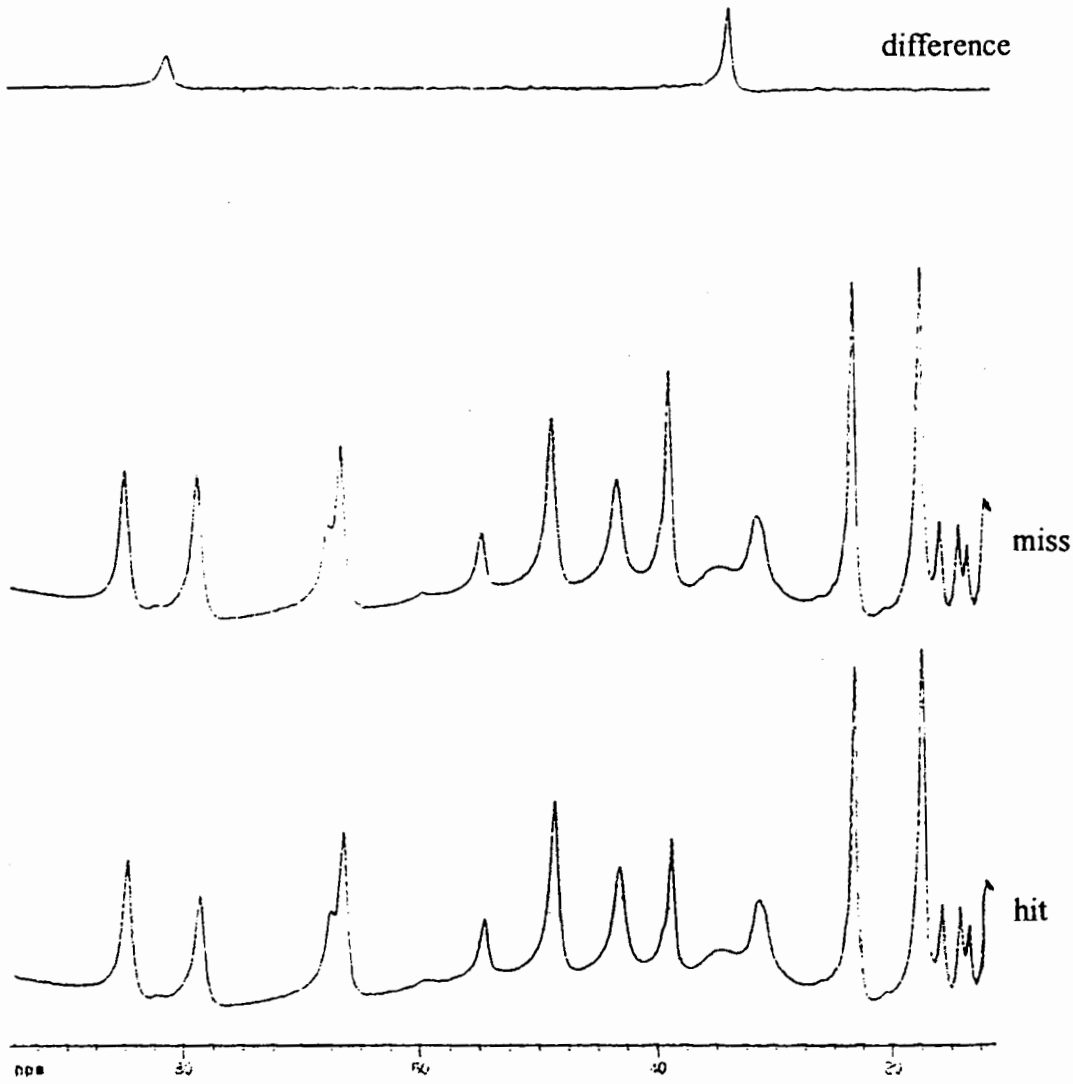

Figure 25. 1D saturation transfer experiment in metMbH_2O / metMb(1MeIm) mixture at 323K.

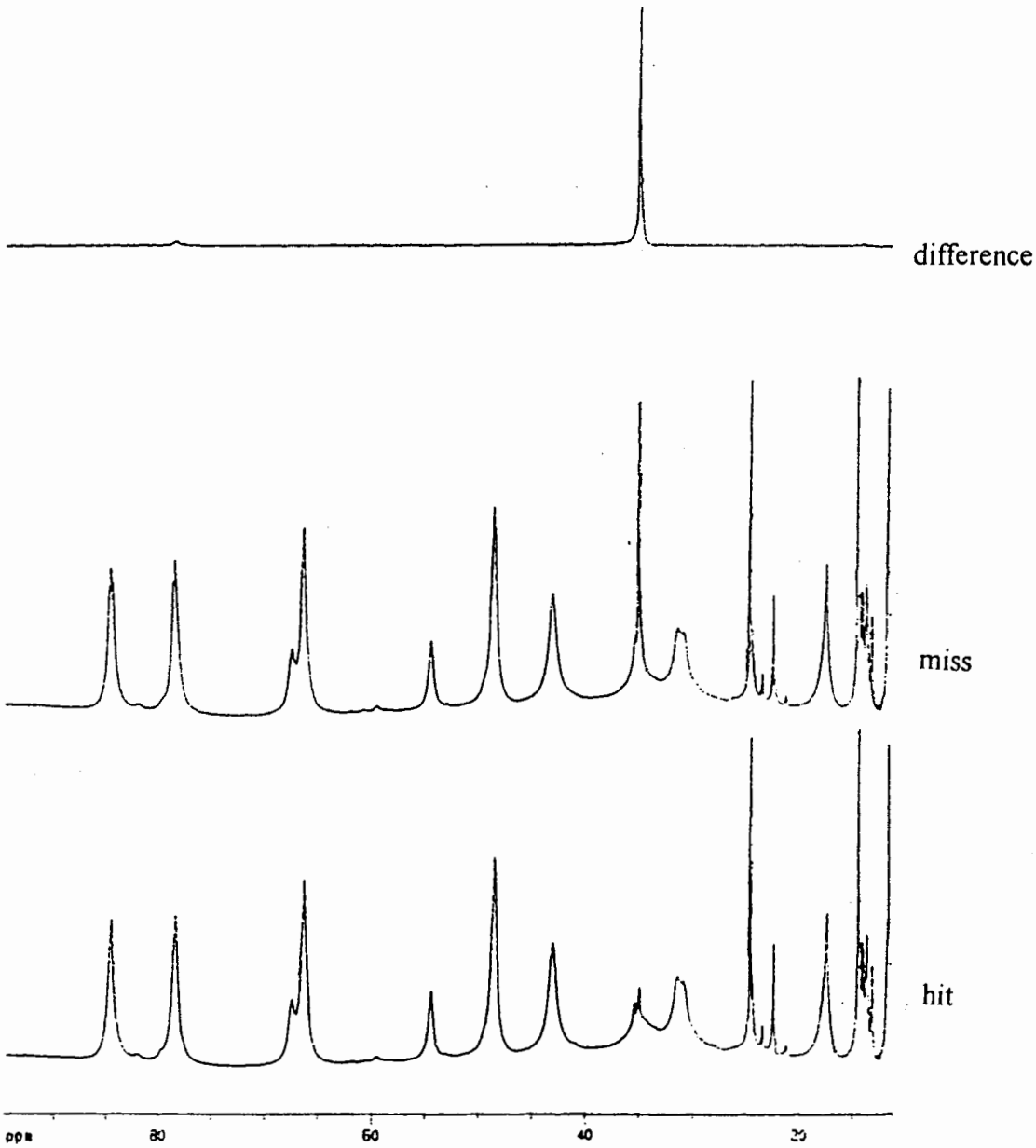

Figure 26. 1D saturation transfer experiment in metMbH_2O / metMb(4MeIm) mixture at 323K.

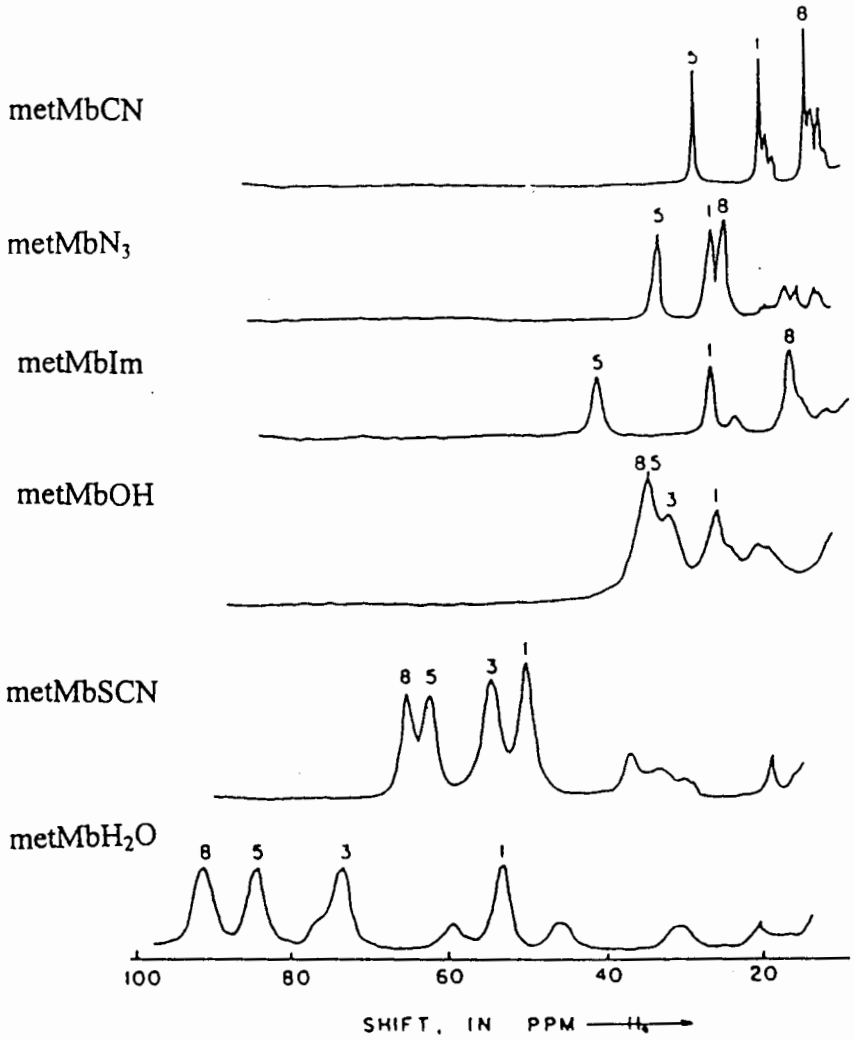

27. Linewidth comparison among myoglobin complexes.

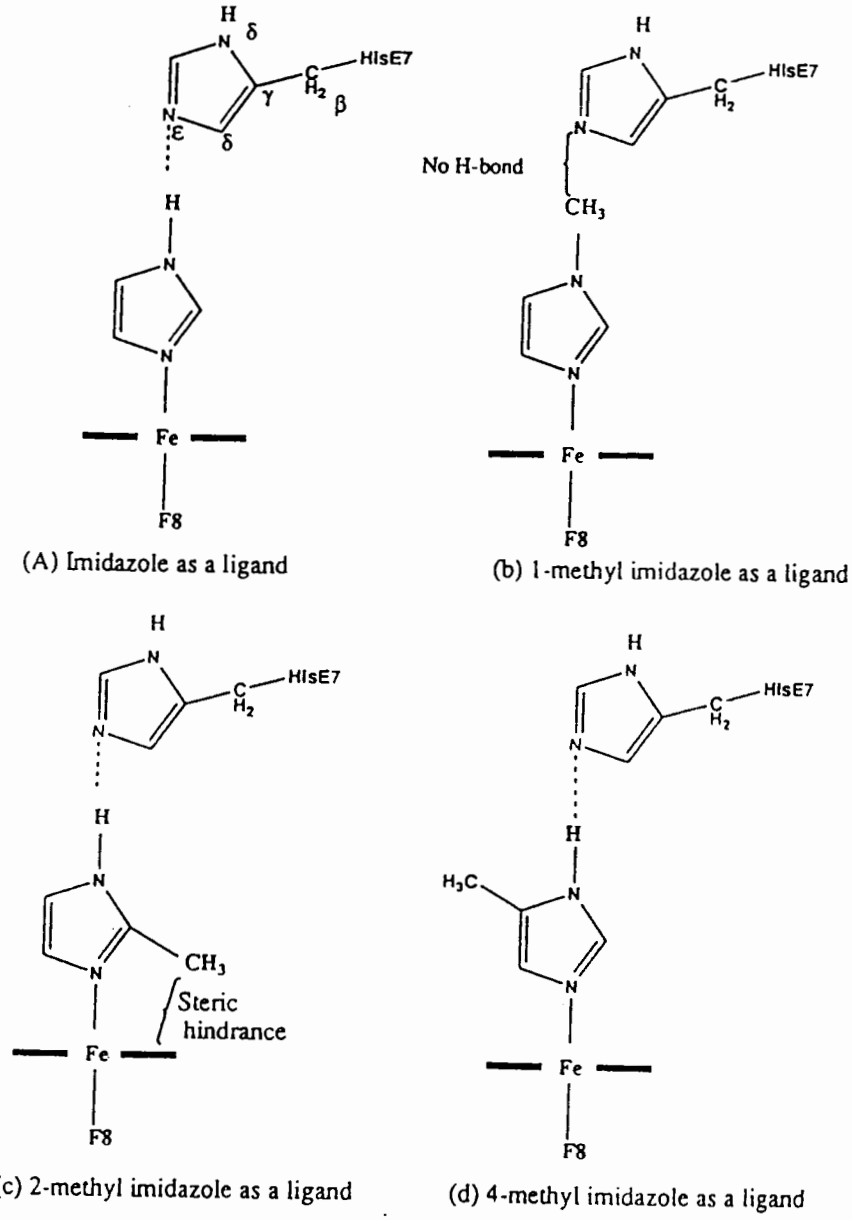

28. Structure of imidazole and methyl substituted imidazoles bound to myoglobin.